Wheat *EARLY FLOWERING3* is a dawn-expressed circadian oscillator component that regulates heading date

Lukas Wittern[1¶], Gareth Steed[1¶], Laura J. Taylor[1], Keith Gardner[2], Andy Greenland[2], Matthew A. Hannah[3], Alex A. R. Webb[1*]

[1]Department of Plant Sciences, University of Cambridge, Downing Street, Cambridge, CB2 3EA, UK

[2]BASF, BBCC – Innovation Center Gent, Technologiepark-Zwijnaarde, Gent, Belgium

[3]NIAB, Huntingdon Road, Cambridge, UK

*Corresponding author

Email: aarw2@cam.ac.uk (AARW)

[¶]These authors contributed equally to this work

Abstract

Optimising the seasonal control of flowering in the major crops is an important component of breeding to match crop adaptation to the target environment. Using an eight parent Multiparent Advanced Generation Inter-Cross (MAGIC) population we investigated the contribution of variation at circadian clock-associated genes to the regulation of heading date in UK and European winter wheat varieties. We identified homoeologues of *EARLY FLOWERING* 3 (*ELF3*) as candidate genes for the *Earliness per se* (*Eps*) *D1* and *B1 loci* in field conditions. We confirmed that a SNP within the coding region of *TaELF3-B1* is the likely causal polymorphism underlying the *Eps-B1 locus.* We also identified that a reported deletion at the *Eps-D1 locus* encompassing *TaELF3-D1,* is in fact a novel allele that lies within an introgression region that contains an inversion relative to the Chinese Spring D genome. Our findings that *ELF3* might be associated with the regulation of heading date prompted us to investigate whether *ELF3* is a circadian oscillator gene in wheat, as it is in Arabidopsis. Using *T. turgidum cv. Kronos* carrying loss of function alleles for both copies of *TtELF3,* we found that circadian rhythms were severely disrupted. Furthermore, in *T. aestivum*, we found that loss of functional *LUX ARRHYTHMO* (*LUX*), an orthologue of the protein partner of ELF3 in Arabidopsis, also severely disrupted circadian rhythms. Whilst these data suggest a function for both *ELF3* and *LUX* in the wheat circadian oscillator, that oscillator might be structured differently to that of Arabidopsis because wheat *ELF3* and *LUX* transcripts are maximal at the end of the night and day respectively, rather than co-expressed at dusk as they are in Arabidopsis. We conclude that there is sufficient allelic diversity within the three wheat *ELF3* homoeologues for selection to delay or advance heading, and that this can be achieved without pleiotropic deleterious alterations to circadian rhythms.

Introduction

Circadian clocks are endogenous timing mechanisms with a near 24 hour period that sequence biological events, provide anticipation of environmental rhythms and permit measurement of daylength to regulate seasonal adjustments (McClung 2019). Plant breeders have indirectly selected for variation at circadian-associated *loci* in many of the world's major crops when breeding to increase yield and improve crop performance by adapting genotypes to the local environment (Steed et al. 2021). Here we investigated whether variation at circadian-associated *loci* contributes to wheat yield traits in the field using a Multiparent Advanced Generation Inter-Cross (MAGIC) mapping population (Mackay *et al.* 2014). Wheat is a major crop, providing approximately 20% of the dietary calories and protein for the world's population (Hawkesford *et al.* 2013). Since the green revolution wheat yields have continued to increase but with the world's population estimated to reach 9.6 billion in 2050 (Gerland *et al.* 2014) it is likely that demand will outpace predicted yield increases (Hawkesford *et al.* 2013). Identification of novel genetic variation contributing to yield is critical to increasing the rate of yield gains in wheat.

Understanding of the nature of plant circadian oscillators is based primarily on investigation of Arabidopsis. In that model, the circadian oscillator contains a series of interlocking transcriptional feedback loops. The circadian oscillator cycle can be considered to start at dawn when expression of the transcriptional repressors *CIRCADIAN CLOCK ASSOCIATED 1* (*CCA1*) and *LATE ELONGATED HYPOCOTYL* (*LHY*) peaks, followed sequentially by peaks of expression of *PSEUDO REPSONSE REGULATOR 9* (*PRR9*)*, PRR7, PRR5, PRR3* and finally *PRR1* (also known as *TIMING OF CAB EXPRESSION 1* (*TOC1*)) at dusk (Hsu and Harmer 2014). PRR9

and PRR7 repress the expression of *CCA1* and *LHY* which releases repression of evening phased genes including, *TOC1, GIGANTEA* (*GI*)*, EARLY FLOWERING 3* (*ELF3*)*, ELF4* and *LUX ARRHYTHMO* (*LUX*) (Hsu and Harmer 2014). LUX is a MYB-like transcription factor which associates with ELF3 and ELF4 to form the tripartite evening complex (EC), which represses expression of *GI, TOC1, PRR7, PRR9* and *LUX* (Dixon *et al.* 2011, Nusinow *et al.* 2011, Herrero *et al.* 2012)*.* Mutation of any of the three EC components causes arrhythmia of the Arabidopsis circadian oscillator in continuous light and temperature (Nagel and Kay 2012).

Orthologues of *ELF3* underlie *loci* regulating heading date in multiple crops, including barley *early maturity8* (*eam8*) (Faure *et al.* 2012), rice *heading date17* (*Hd17*) (Matsubara *et al.* 2012), *Earliness per se* (*Eps*)-A^{m}*1* in *T. monococcum* and *Eps-D1* in *T. aestivum* (Zikhali *et al.* 2016). In hexaploid wheat, the magnitude of the *Eps-D1* effect on heading date increases with decreasing temperature (Ochagavía *et al.* 2019). Orthologues of *TOC1* are associated with heading date, plant height and thousand grain weight (Sun *et al.* 2020). An orthologue of *LUX* is a candidate for *Eps-3*A^{m} in *T. monococcum* (Gawronski *et al.* 2014) and *HvLUX* is a candidate gene for *eam10* in barley (Campoli *et al.* 2013). Furthermore, the *Photoperiod-1* (*Ppd-1*) genes*,* which contribute to photoperiodic regulation of ear emergence, are orthologues of Arabidopsis *PRRs* (Beales *et al.* 2007, Shaw *et al.* 2012, Bentley *et al.* 2013, Turner *et al.* 2013).

We used the allelic diversity of a wheat MAGIC population to investigate the role of circadian clock genes in regulating yield component traits in the field. The founder varieties for the MAGIC population used in this study (Alchemy, Brompton, Claire, Hereward, Rialto, Robigus, Soissons and Xi-19) are representative of UK and

European winter wheat varieties, capturing >80% of the polymorphism found across UK wheat varieties from the last 70 years (Gardner *et al.* 2016). Our data suggest that breeding for modified *ELF3* function can affect the regulation of flowering time but potentially without compromising yield through disrupted circadian oscillations. We find evidence of differences in the role for ELF3 in the circadian system between wheat and Arabidopsis by concluding that in wheat, *ELF3* is expressed in the morning, rather than the evening.

Results

Earliness per se *loci Eps-B1* and *Eps-D1* segregate in an eight-parent wheat MAGIC population

We performed QTL analysis on a set of replicated trial data for 784 recombinant inbred lines (RILs) for the NIAB Elite MAGIC population from the 2012/2013 and 2013/2014 growing seasons at the NIAB experimental farms in Cambridge, UK. Growth stage 55 (GS55, equivalent to heading date) (Zadoks *et al.* 1974) was chosen for analysis and QTL mapping to enable comparisons with previous studies (Griffiths *et al.* 2009). In both 2013 and 2014, Soissons, which contains the *Ppd-D1a* (photoperiod insensitive) allele, reached GS55 6-8 days earlier than any of the other MAGIC parents, which contain the *Ppd-D1b* allele (photoperiod sensitive) (Fig 1). Heading date of the other MAGIC parents varied over 5.5 days in 2013 and 7 days in 2014.

We performed the QTL analysis using MPWGAIM (Verbyla *et al.* 2014) for GS55 phenotypes in both years and tested whether any circadian clock genes co-locate with the identified QTLs (< 2 cM to nearest 90 k marker or < 5 Mb to gene). Because

we are interested in the effects of circadian clock on yield, we report only QTLs associated with circadian clock genes. We found that four circadian gene orthologues (*TaELF3-B1, TaELF3-D1, Ppd-1, TaZTL-7A*) fell within 0.20, 0.27, 0.58 and 4.31 Mb respectively of one of the QTL flanking markers (Table 1). The absence of significant heading date QTLs linked to vernalisation genes such as *VRN1* confirmed that complete vernalisation had occurred, ensuring that observed variations in heading date were true *Earliness per-se* (*Eps*) effects rather than a variation in the vernalisation requirements between the MAGIC parents (Bentley *et al.* 2013, Camargo *et al.* 2016). A previous study identified a single GS55 QTL in the NIAB eight parent MAGIC population (Camargo *et al.* 2016) but this difference in findings is likely a result of different growth conditions (greenhouse compared to field), lower replicate number (208 RILs in pots compared to 784 RILs in field plots) and the use of a different mapping methodology. Further validation of our analysis pipeline and approaches are described in the methods and reported in (S1 Table).

A QTL on the distal end of chromosome 1B, delineated by the markers Ra_c109187_371 and RAC875_c37075_283, mapped closely to the physical position of *TaELF3-B1* (TraesCS1B02G477400) (Table 1). The 1B locus also had a homoeologous QTL on chromosome 1D delineated by the markers Kukri_c29687_369 and Kukri_rep_c69829_307 identifying *TaELF3-D1* (TraesCS1D02G451200) as a candidate gene (Table 1, Fig 2A). These QTLs co-locate with the previously described heading date QTLs *Eps-B1* and *Eps-D1* (Griffiths *et al.* 2009). In our data, *Eps-B1* had a significant effect in both years, explaining 3.4% of genetic variance in GS55 in 2013 and 2% in 2014 (Table 1). *Eps-D1* was also detected in both years but only had an overall significant effect (–log10(p) = 2.32) in 2014, accounting for 4.1% of genetic

variance in GS55 in that year (Table 1). The *Eps-B1* and *Eps-D1 loci* were chosen for further in-depth analysis because of their proximity to *ELF3* homoeologues.

TaELF3-B1 is a candidate gene for the *Eps-B1* QTL

At the 1B QTL, the alleles derived from the MAGIC founders Soissons, Alchemy, Robigus and Claire caused a relative reduction in the time to GS55, indicated by the negative sign of the QTL, whilst alleles from Rialto, Hereward, Xi-19 and Brompton caused a delay to GS55, indicated by the positive sign of the QTL (Table 2). The interval between the markers Ra_c109187_371 (296.34cM / 685.7Mb) and RAC875_c37075_283 (297.00cM / 687.7Mb) is 0.66cM, corresponding to a physical length of ca. 2 Mb (Fig 2A).

The IWGSCv1.1 gene annotation suggests there are 26 high confidence gene models within the interval of Ra_c109187_371 and RAC875_c37075_283. Based on current gene annotation and orthology to cloned rice genes (Yao *et al.* 2018) there are no novel candidates for the *Eps-B1* locus in addition to those described previously (Faricelli *et al.* 2010, Alvarez *et al.* 2016, Zikhali *et al.* 2016). Compared to the *T. monococcum* physical map of the *Eps-A^{m}1* region (Alvarez *et al.* 2016) *TmADK* (similar to rice putative kinase *ADK1)* and *TmCK1-like* (*CASEIN KINASE I ISOFORM DELTA-LIKE)* are not syntenic and the locus containing *TaELF3*, *TaGRIK1-like* (*GEMINIVIRUS REP INTERACTING KINASE 1 LIKE*) and *TaPWWP1* (*PWWP domain-containing protein*) is inverted (Fig 2A). Nineteen genes had homoeologues on the syntenic 1D chromosome (Fig 2A).

Publicly available sequences for *TaELF3-B1* in Claire, Robigus (earlier heading alleles) (Clavijo *et al.* 2017) and Rialto and Cadenza – the parents of Xi-19 - (later heading alleles) (Zikhali *et al.* 2016) differed by one non-synonymous SNP within exon 4 at position chr1B:685645813. No further nonsynonymous SNPs were identified from the 820k SNP dataset from CerealsDB (Wilkinson *et al.* 2012), which contains all MAGIC parents.

The SNP (Adenine at position 2020 of CDS to Guanine; A2020G) causes a predicted deleterious amino acid substitution from the ancestral serine to a glycine residue at position 674 of the predicted primary amino acid sequence (Ser674Gly; SIFT 0.01) (Fig 2B). A KASP marker was designed for this SNP and used to genotype the MAGIC population. The KASP marker mapped to the same genetic position as Ra_c109187_371 and segregated with the predicted founder effects, confirming that *TaELF3-B1* is part of the 1B GS55 QTL.

A predicted glycine at residue 674 of *TaELF3-B1*, associated with late heading, is globally rare in wheat. In the 1000Exome data (He *et al.* 2019) 4.87% of lines have the predicted glycine residue and in the wheat HapMap panel (Jordan *et al.* 2015), only Rialto has the predicted glycine residue out of the 62 globally diverse lines analysed (S2 Table). Similarly, of the 14 hexaploid varieties currently available from the 10+ Wheat Genome project only three (Cadenza, Paragon, ArinaLrFor) possess the non-ancestral glycine residue (S2 Table). However, analysis of multiple datasets (see methods) shows the non-ancestral glycine674 is more common in wheat varieties with a UK pedigree (9/13 varieties) (S3 Table). Alignment of *TaELF3* orthologues

shows that the predicted serine residue is also highly conserved across monocots (S1 Fig).

When looking for other potentially causal sequence variation we found that within the *ELF3-B1* promoter regions of Claire, Robigus, Paragon and Cadenza there are two sites polymorphic for the number of repeated cytosines ($(C)_n$) located 1967 bp and 1151 bp upstream of the transcriptional start site (TSS) (Fig 2B). As Robigus and Claire have an early heading phenotype at the *Eps-B1* locus and Cadenza a late heading phenotype (Alvarez *et al.* 2016) it is unlikely that the promoter $(C)_n$ polymorphisms cause the changes in heading dates because there is only a difference in two cytosines at the 1967 bp $(C)_n$ site between Cadenza and Robigus/Claire (Fig 2B). Furthermore *TaELF3-B1* on Julius, Lancer, Mace, Norin61 and Sy Mattis seem to be inverted compared to ArinaLrFor, CDC Landmark, CDC Stanley, Chinese Spring and Jagger. However, as none of these lines share the same haplotype with ArinaLrFor and Paragon (which both carry the Ser674Gly SNP) at *ELF3-B1* it is unlikely that an inversion is the cause behind the *Eps-B1* QTL. Thus, we conclude that the Ser674Gly SNP in *ELF3-B1* is the best candidate to underlie *Eps-B1*.

Subtelomeric introgression and inversion might underlie the *Eps-D1* heading date QTL

A subtelomeric deletion in Cadenza and Spark was previously described as the causal polymorphism underlying the *Eps-D1* locus using Spark × Rialto, Avalon × Cadenza mapping populations (Zikhali *et al.* 2016, Ochagavía *et al.* 2019). Our QTL analysis for 2012 (S1 Table) and 2014 (Table 1) shows a minor QTL overlapping this locus. In both years the Xi-19 founder genotype is associated with earlier flowering (2012: -1.26

days; p = 0.015; 2014; -0.79 days; p = 0.053). However correct genetic map construction and resulting assignment of founder genotypes at this locus might be more difficult given the high-density marker region previously identified at the end of 1D. These high-density marker regions were hypothesised to be associated with introgressions (Gardner et al., 2016). Based on the previously reported deletion in Cadenza and Spark (Zikhali, Wingen, and Griffiths 2016) and the pedigree of Xi-19 (Cadenza/Rialto//Cadenza) we hypothesised that the Cadenza allele inherited from Tonic was a likely candidate for the observed QTL effects. By analysing data from recently published wheat assemblies (Walkowiak *et al.* 2020) we suggest the polymorphism is due to a subtelomeric inversion derived from introgressed material rather than a deletion. A BLAST search of the Chinese Spring *TaELF3-D1* genomic sequence against the 10+ Wheat Genome Project varieties identified high confidence matches in all varieties including Cadenza. Interestingly, the sequence retrieved from the variety Jagger was identical to Cadenza. However, the sequence identity of the Jagger and Cadenza coding sequence for TraesJAG1D01G492900.1 and TraesCAD_scaffold_026352_01G000400.1 compared to the Chinese Spring gene is much lower (96.72%) than for the remaining 1D coding sequences (>99.9%). The Jagger and Cadenza 1D coding sequences have a greater similarity to the Chinese Spring *TaELF3-A1* (97.50%) and Chinese Spring *TaELF3-B1* (97.88%) homoeologues than to Chinese Spring *TaELF3-D1*.

Visualisation of the 1D chromosome for the 10+ Wheat Genome Project varieties using the Crop Haplotypes viewer (Brinton *et al.* 2020) showed a shared haplotype block at the distal end of chromosome 1D between Cadenza (Haplotype viewer coordinates:

482.8 Mbp – 495.4 Mbp) and Jagger (480.0 Mbp to 493.5 Mbp) where *TaELF3-D1* is found.

The Cadenza v1.1 reference sequence has yet to be assembled into chromosomes, but since the Crop Haplotypes viewer (Brinton *et al.* 2020) data indicated identical by state (IBS) haplotypes between Jagger and Cadenza, we compared the distal end structure of the Jagger 1D chromosome with Chinese Spring. The end of the Jagger chromosome contains an inversion of approximately 2.6 Mbp relative to Chinese Spring which includes *TaELF3-D1* (Fig 3A). Alignment of the Jagger/Cadenza *TaELF3-D1* genomic sequence with Chinese Spring *TaELF3-D1* showed some sequence differences including a deletion within intron 2 (Fig 3B, S4 Table). We developed a subgenome specific PCR assay detailed in Fig 3B that amplifies the region of *TaELF3-D1* containing intron 2 and confirmed that of the eight MAGIC parents, only Xi-19 carried the Cadenza/Jagger *TaELF3-D1* allele (Fig 3C and D). As hypothesised Spark and Tonic also carry the Cadenza *TaELF3-D1* allele (Fig 3C, D and S2 Fig) as well as the varieties Maris Fundin and Cordiale. The intron 2 deletion is also present in *Aegilops speltoides* and *Triticum timopheevii* (S3 Fig).

Given the low sequence conservation of the *TaELF3-D1* gene in Cadenza and Jagger and the presence of the intronic deletion in *Aegilops speltoides* and *Triticum timopheevii*, we investigated the wider phylogeny of the 1D Jagger/ Cadenza region using the 820k SNP dataset from CerealsDB. This showed that Cadenza, Xi-19 and Spark as well as several other Tonic descendants (KWS-Podium, Cordiale, Gallant, Duxford) and five other cultivars (Moisson, Bacanora, Tuerkis, Badger, Pavon) clustered separately from the remaining *T. aestivum* cultivars (S4 Fig). These lines

also cluster with six Watkins lines from India (Watkins34), Yugoslavia (Watkins352), China (Watkins141), UK (Watkins103), Cyprus (Watkins292) and Turkey (Watkins299). *T. timopheevii* clusters closely with the above lines. Gene alignment of *ELF-D1* orthologues and alignment of 300kb surrounding *ELF3-D1* also supports an origin outside the D genome for the Jagger/ Cadenza *ELF3-D1* gene (S5 Fig, S5 Table).

Allelic variation in *TaELF3* had no detectable effect on circadian rhythms in the MAGIC founder varieties

We investigated if the variations at *TaELF3-B1* and *TaELF3-D1* in the MAGIC parents, or other *loci,* might affect circadian rhythms in a manner that might explain the effects on heading date. We quantified circadian rhythms in the MAGIC founder varieties by measuring the period and amplitude of rhythms of delayed chlorophyll fluorescence (DF) in otherwise constant light (Gould *et al.* 2009). We detected robust circadian rhythms of DF in all the MAGIC parent lines (RAE < 0.5) (Fig 4A). Hereward had the shortest circadian period (25.0 h) (Fig 4C) and Xi-19 the longest period (26.2 h) but the difference between these periods and the global mean was not significant ($p = 0.132$) (Fig 4C). Thus, the allelic diversity in homoeologues of *TaELF3* did not cause detectable changes in circadian rhythms.

Loss of function mutation of *TtELF3* disrupts wheat circadian clocks

Because we found that variation in the MAGIC parents at *TaELF3* was not correlated with a detectable effect on circadian rhythms, we examined whether *ELF3* is a

circadian oscillator component in wheat. We obtained a tetraploid TILLIING mutant line carrying point mutations encoding stop codons in both *TtELF3-A1* and *TtELF3-B1* (Alvarez *et al.* 2016) herein designated *Ttelf3*-null (S6 Fig). We quantified circadian rhythms of "prompt" chlorophyll *a* fluorescence (PF) (Dakhiya *et al.* 2017) and leaf temperature under continuous light in both the *Ttelf3*-null and the respective *TtELF3*-WT obtained from the initial mutant TILLING line (Alvarez *et al.* 2016). We detected circadian rhythms in *TtELF3*-WT but *Ttelf3*-null was arrhythmic for all measures of PF (Fig 5C and S7 Fig) including $F_{m'}$ (*TtELF3*-WT RAE 0.36 ± 0.03; *Ttelf3*-null RAE 0.82 ± 0.08) (Fig 5C), leaf temperature (*TtELF3*-WT RAE 0.20 ± 0.04; *Ttelf3*-null RAE 0.56 ± 0.10) (Fig 5D-F) and DF (S8 Fig). The mean peak phase of relative leaf temperature for *TtELF3*-WT (Fig 5D) was 20.0 ± 0.2 h after subjective dawn, indicating, as expected, that stomata were most closed during the middle of the subjective night.

Loss of functional *TtELF3* perturbs circadian oscillator gene expression in light/dark cycles and constant light

To further investigate the function of *ELF3* in the wheat circadian system we measured the abundance of transcripts of orthologues of the Arabidopsis circadian oscillator components *LHY, TOC1, Ppd-1* (*PRR37*)*, PRR73, GI, ELF3* and *LUX* in light dark (LD) and continuous light (LL) cycles. In LD cycles all transcripts had rhythmic expression (Fig 6A-G). Consistent with previous findings in Arabidopsis, *TtLHY* had peak expression at dawn (Fig 6A), the *PRR* orthologues peaked during the photoperiod (Fig 6B-C) with *TtTOC1* (Fig 6D), *TtGI* (Fig 6E) and *TtLUX* (Fig 6F) peaking around dusk. However, the peak in *TtELF3* abundance was at the end of the night just prior to dawn (Fig 6G), approximately antiphase to the expression of *TtLUX* (Fig 6F). This differs markedly from Arabidopsis in which *ELF3* and *LUX* are co-

expressed near dusk (Nusinow *et al.* 2011, Huang *et al.* 2016, Ezer *et al.* 2017). For all transcripts, except *Ppd-1* (Fig 6B), we detected oscillations in transcript abundance in constant light, with the phasing in LL consistent with that in LD. These oscillations of circadian transcript abundance were abolished, or of very low amplitude, in *Ttelf3*-null (Fig 6A-G). There was a phase advance in peak transcript abundance of approximately 3 h in LD in *Ttelf3*-null compared to *TtELF3-WT* (Fig 6A-G) except for *TtELF3* transcript abundance where the peak phase was at dawn in both *TtELF3*-WT and *Ttelf3*-null (Fig 6G). The amplitude of transcript abundance under diel conditions was also less in the *Ttelf3*-null line compared to *ELF3*-WT (Fig 6). Together, these data demonstrate that functional *TtELF3* is required for the maintenance of robust oscillations of circadian oscillator gene expression in LL and for normal circadian timing in LD.

LUX loss of function disrupts the wheat circadian clock

The antiphase expression of wheat *ELF3* and *LUX* raises the possibility that the EC might not be formed, or functions differently to that in Arabidopsis. Previous studies in diploid wheat have identified *TmLUX* as a circadian oscillator gene (Gawronski *et al.* 2014), so we investigated whether *LUX* also contributes to circadian rhythms in hexaploid wheat, and whether functionality of one homoeologue is sufficient to maintain robust oscillations. We obtained three hexaploid Japanese cultivars, Chogokuwase, Minaminokomugi and Geurumil that have variation at *TaLUX* associated with flowering time (Mizuno *et al.* 2012). Chogokuwase is an extra early flowering variety and is the offspring of Geurumil and Minaminokomugi. Chogokuwase carries predicted non-functional mutations in all three sub-genome copies of *TaLUX* (S9 Fig). Chogokuwase also carries a *TaVRN-D1* spring allele and a photoperiod

insensitive *Ppd-D1a* allele. Geurumil has the same predicted non-functional alleles of *TaLUX* and *Ppd-D1a* but has a winter growth habit due to lacking the *VRN-D1* spring allele. Minaminokomugi carries the non-functional *Talux-a1* allele but wild-type alleles of *TaLUX-B1* and *TaLUX-D1* in addition to carrying the *TaVRN-D1* and *Ppd-D1a* alleles (Mizuno *et al.* 2016).

Minaminokomugi maintained robust oscillations of chlorophyll fluorescence (RAE 0.16 ± 0.01) and leaf temperature (RAE 0.26 ± 0.02) (Fig 7A-C). In contrast Chogokuwase, which lacks functional copies of *TaLUX,* was arrhythmic for PF (RAE 0.56 ± 0.06) and Geurumil, which is also lacking functional *TaLUX*, had reduced robustness of PF oscillations (RAE 0.33 ± 0.05) compared to Minaminokomugi (Fig 7A-C). Similarly, there was a decreased robustness of oscillations in leaf surface temperature for Chogokuwase and Geurumil (RAE 0.48 ± 0.09 and RAE 0.46 ± 0.11) which appeared to dampen to arrhythmia after the first two true LL cycles (Fig 7D-F). We conclude that functional *TaLUX* is required for robust circadian rhythms in hexaploid wheat.

Discussion

Wheat *ELF3* contributes to heading date and circadian rhythms

The eight MAGIC parent varieties provided the opportunity to measure the likely contribution of the *ELF3* homoeologues to heading date and circadian rhythms. Of the MAGIC parents Brompton, Hereward, Rialto and Xi-19 have a G|G substitution variant of *TaELF3-B1* and in addition Xi-19 has an inverted copy of *TaELF3-D1,* likely arising from a past introgression event. These variations in *TaELF3* alleles had no discernible

impact on circadian rhythms (Fig 4) but had measurable effects on heading date in the field (S10 Fig).

Consistent with previous studies, we conclude that *ELF3* underlies *Eps-B1* and is a candidate for *Eps-D1 loci* (Zikhali *et al.* 2016). We have extended the findings concerning the *Eps-D1* locus by demonstrating that a copy of *ELF3-D1* is present in Cadenza (as well as Xi-19, Spark, Cordiale, Tonic and Maris Fundin) but lies within an introgression region that contains an inversion relative to the Chinese Spring D genome (Fig 3). Based on analysis of the 820k SNP data we find that a number of descendants of the cultivar Tonic carry the putative introgression, as do several other unrelated cultivars and six Watkins lines from India, China, UK, Cyprus, Turkey and Yugoslavia. The introgression is also likely present within Chinese elite germplasm (Wang *et al.* 2016). As a result, we hypothesise that this region predates modern breeding efforts. The same genomic region has been identified as being under selection in a collection of bread wheat accessions dating from 1790 to 1930, though in that study it was presumed to be a deletion rather than introgression (Przewieslik-Allen *et al.* 2021). While the origin of the introgression is uncertain, the presence of Jagger/Cadenza *TaELF3-D1* intronic deletion in *Ae. speltoides* and *T. timopheevii* (S3 Fig) and the clustering outside of *Aegilops tauschii* lines (S4 and S5 Figs) supports an origin outside of the D genome, more closely related to the G or S genome. The increase in quantity and quality of genomic resources for diverse accessions and wheat relative species will help in determining the origin of this introgression.

Our data also identify *TaELF3-B1* as a candidate gene underlying the *Eps-B1* locus. We found that a predicted glycine674 in *TaELF3-B1,* which segregates with *Eps-B1,*

caused a delay in heading and flowering compared to the ancestral serine674 variant (S10 Fig), in agreement with previous observations in Avalon (Zikhali *et al.* 2016). It was previously concluded that G|G is the ancestral variant (Zikhali *et al.* 2016) but our evidence suggests that it is more likely that A|A is ancestral because the G|G allele is globally rare, present in 4.87% of lines included in the 1000 Exome dataset, in one of the 62 wheat HapMap panel lines (S2 Table) and in three of the 14 10+ Wheat Genome project lines (S2 Table) and the ancestral serine residue is highly conserved, present in all sequenced grasses. However, within UK wheat germplasm (as defined by locality on wheat GRIS) the G|G allele is more common and is found in nine of the 13 UK lines we have investigated (S3 Table). The later flowering G|G allele may be more favoured in northern regions (Langer *et al.* 2014).

We found that the allelic variation at *TaELF3* had no detectable effect on circadian rhythms in the MAGIC founders. Epistasis between *ELF3* and *Ppd-D1* has previously been reported for flowering time (Faure *et al.* 2012, Alvarez *et al.* 2016). However, we find that variation at *Ppd-A1* has no obvious effects on circadian rhythms or modification of circadian phenotypes in *Ttelf3* nulls (S11 Fig). We also find no evidence of epistasis between *eps-B1* and *eps-D1* in regulation of circadian rhythms because Xi-19 has both *eps-B1* and *eps-D1* but was not distinguishable from the rest of the population in terms of circadian behaviour.

Only complete loss of functional *TtELF3* caused arrhythmia of PF (Fig 5A-C & S7 Fig), leaf temperature (Fig 5D-F) and gene expression in LL (Fig 6), and this loss of function caused advanced circadian phase in LD. This demonstrates that one role of *ELF3* is to contribute to the correct alignment of internal phase to external phase, which is a

primary function of circadian oscillators. The earlier phasing of gene expression in LD cycles is similar to barley containing the *eam8.*w allele where the peak phase of *HvCCA1, HvTOC1* and *HvGI* expression was also earlier (Faure *et al.* 2012). Similarly, the same study reported loss of rhythmic oscillations in gene expression upon transition to LL in barley. We found that functional *TtELF3* is required for high amplitude *TtLHY* rhythms, and that *TtELF3* loss of function mutants have increased trough transcript abundance of *TtGI* (Fig 6E). The similarity of these observations to those in barley and rice lines carrying *ELF3* mutations (Zhao *et al.* 2012, Boden *et al.* 2014) suggests that *ELF3* genes might have similar functions across grasses.

An altered role for the evening complex (EC) in wheat

Binding of the Arabidopsis EC to target promoters requires LUX as both ELF3 and ELF4 lack DNA binding domains, and it is thought this might explain the similar timing of the transcript accumulation (Nusinow *et al.* 2011). However, in wheat the maximal abundance of *ELF3* and *LUX* transcripts is separated by 12 hours (Fig 6F and G). This difference in the peak time of *ELF3* and *LUX* transcript abundance also occurs in *T. monococcum* (Alvarez *et al.* 2016) and rice (Zhao *et al.* 2012) and therefore may be a general feature of cereal circadian oscillators. Wheat also lacks a clear orthologue of *AtELF4* and instead contains *ELF4-like* genes (Calixto *et al.* 2015). *ELF4-like* genes might have a conserved role because expression of a barley *ELF4-like* gene restored circadian rhythms to an Arabidopsis *elf4-2* mutant (Kolmos *et al.* 2009). There is further evidence for conservation of EC function in monocots because Brachypodium ELF3 binds Arabidopsis ELF4 and LUX, and can complement Arabidopsis *elf3-2* mutants (Huang *et al.* 2017). The temporal separation of wheat *ELF3* and *LUX* transcript abundance does not preclude the formation of an EC complex, but could

suggest one is not formed, or occurs at a different time in the diel cycle to Arabidopsis. Whether through an EC or not, our data demonstrate that functional *ELF3* and *LUX* are required for robust circadian rhythms in wheat (Figs 6- 8).

The difference in timing of *TaELF3* and *TaLUX* expression compared to their Arabidopsis orthologues might arise as a consequence of promoter sequence differences. Within 5000 bp upstream of the three *TaELF3* homoeologues transcription start sites the most common motifs are linked to morning phased expression (37 morning, 20 evening and 7 midnight) (S6 Table). The general composition of the *TaELF3* promoters is similar to *TaLHY* (22 morning, 9 evening and 3 midnight) (S7 Table) but different to the evening expressed *TaLUX* promoters where the most abundant motifs are associated with evening phased expression (32) compared to morning (23) and midnight (12) (S8 Table). In particular*, TaELF3* promoters contain Morning Element 1 (ME1) and Morning Element 2 (ME2) motifs, associated with morning phased expression (Michael *et al.* 2008), which are also found in the promoter region of the dawn expressed *TaLHY* homoeologues (S7 Table) but are absent in the *AtELF3* promoter (S6 Table). The *TaELF3* promoters also contain further morning-related motifs such as the multiple Hormone up at dawn 1 (HUD1) and Hormone up at dawn 2 (HUD2) elements (Michael *et al.* 2008) which are less frequent in the *AtELF3* promoter (S6 Table).

Wheat *ELF3* might be a promising breeding target

ELF3 might be a suitable target for breeding new lines with heading date better adapted to the local environment in the practice of chronoculture (Steed *et al.* 2021). In other species such as pea, lentil and barley, allelic variation in *ELF3* has permitted

the cultivation of these crops at different latitudes (Weller *et al.* 2012, Zakhrabekova *et al.* 2012, Lundqvist 2014). Whilst complete loss of functional *ELF3* in wheat significantly advances flowering time, severely disrupts circadian rhythms and decreases the spikelet number (Alvarez *et al.* 2016), we have demonstrated that altering the function of particular homoeologues of *ELF3* can affect heading without a measurable disruption to the circadian oscillator and the potential associated yield penalties (Dodd *et al.* 2005) if some functional copies of *ELF3* are present. It might be possible that by combining different alleles of *ELF3* with alleles of other circadian clock genes, flowering time can be precisely tuned to suit the growing environment. This could be tested by measuring flowering time in selected Cadenza TILLING lines (Krasileva *et al.* 2017) containing mutations in other circadian clock genes as Cadenza contains both the *TaELF3-B1* Ser674Gly SNP and the 1D introgression. In addition to the *ELF3* alleles described in this work, we have also identified further *ELF3* alleles including the absence of *ELF3-A1* in Julius (S9 Table) highlighting a range of *ELF3* alleles within modern wheat cultivars which could be incorporated into breeding programmes. The variation at *ELF3* might have occurred because of the positioning of *ELF3* within the subtelomeric region (Aguilar and Prieto 2020) which has enhanced levels of recombination which can lead to increased number of sequence and structural variants. This has been observed for other regions, recent studies have reported that a deletion at the distal end of chromosome 4AL is associated with altered heat tolerance (Zhai *et al.* 2021) and a deletion at the distal end of 5AL encompasses the *Rht12* locus which is associated with dwarfing (Sun *et al.* 2019). Secondly, variation at *ELF3* may have been selected by past breeding efforts, leading to a change in allele frequencies, due to advantageous adaptation of flowering time to local climates similar to that seen for selection of *Ppd-1* alleles based on latitudinal cline

(Cockram *et al.* 2007) and altitude (Guo *et al.* 2020). A more systematic understanding of circadian clock gene alleles and their combinations will allow for a more targeted approach in optimising flowering time without impacting the functioning of the circadian clock.

Materials and methods

Plant material

The eight MAGIC parents; Alchemy, Brompton, Claire, Hereward, Rialto, Robigus, Soissons and Xi-19 were obtained from NIAB (National Institute of Agricultural Botany, UK). The *Ttelf3*-null and *TtELF3*-WT lines were donated by Jorge Dubcovksy (Alvarez *et al.* 2016) where the *Ttelf3*-null line is the progeny of bulked *elf3-null/Ppd-A1b* and the *TtELF3*-WT line is progeny of bulked *ELF3WT/Ppd-A1b* (Table 4). The Chogokuwase, Minaminokomugi and Geurumil lines were donated by Hidetaka Nishida (Mizuno *et al.* 2012).

Plant growth conditions

Seeds were surface sterilised by washing once in 70% (v/v) ethanol for one minute (Fischer Scientific, UK), once in autoclaved water for one minute, followed by 15 minutes in 10% (v/v) sodium hypochloride solution (Fischer Scientific, UK) and then washed a further three times in autoclaved deionised water. Seeds were sown directly onto 96 well modular trays (P G Horticulture Ltd, UK), containing a 1:1 mix of Levington M2 potting compost (Levington, UK) and vermiculite (fine, Willian Sinclair Horticulture, UK) and treated with the insecticide Intercept 70W (0.02 g L-1 soil, Bayer, Germany).

Plants were grown in growth chambers (Conviron, Canada) under long days and constant temperature (16 h L: 8 h D; 200 µmol m^{-2} s^{-1}; 20 °C).

Field trials

In 2012/2013 a fully replicated yield trial of 784 F_5 MAGIC lines at the NIAB experimental farm in Cambridge, UK was scored by NIAB for the timing of Growth Stages on the Zadok's scale (Zadoks *et al.* 1974, Mackay *et al.* 2014). Each plot was assessed every two days for its growth stage based on representative plants at the centre of each plot. Once a plot reached GS55 (half of ear emerged above flag leaf ligule) the date was logged. The phenotype was assessed with growth stage measurements scored as days after sowing. In the 2013/2014 field season the same growth stage phenotypes were collected from a fully replicated yield trial of 784 F_6 MAGIC lines.

Analysis of field phenotypes

Asreml-R 3.0 (Gilmour *et al.* 1997) was used to minimise or remove spatial effects in phenotype data due to field variation.

Marker genotypes and their respective chromosomal groupings from (Gardner *et al.* 2016) were used. The genetic map was reordered visually using the R package mpMapInteractive (Shah 2013) to improve ordering and consider physical ordering information from IWGSCRefSeqv1. Recombination fractions were recalculated in mpMap (Huang and George 2011) for each chromosome using mpestrf(). Recalculating recombination fractions on a per chromosome basis with the existing marker groupings significantly reduced computation resources required and enables

the use of finer recombination bins (r <- c(0:5/600, 2:20/200, 11:50/100) compared to the default values. Genetic map lengths were recalculated using the Kosambi mapping function in computemap().

To reduce computational effort a skimmed genetic map with only unique mapping locations was used to calculate the probability that each location on a genome was inherited from each founder and conduct QTL mapping in MPWGAIM only (Verbyla *et al.* 2014). A marker for each unique coordinate was chosen which had the lowest missing calls and preferably a clear BLAST hit to the IWGSCRefSeqv1 reference sequence, which was used to assign physical mapping coordinates. Out of 18089 mapped markers 4458 were chosen for founder probability calculations.

To test and validate our pipeline and analysis tools we used them to interrogate a data set describing flowering time in a 2011/2012 nursery of the NIAB eight Parent MAGIC population that had previously been analysed using Bayesian Networks (Scutari *et al.* 2014). Reanalysis of this data using MPWGAIM (Verbyla *et al.* 2014) detected 13 significant QTLs for flowering time with significant founder effects (S1 Table).

This analysis identified a major QTL (18.3% genetic variation explained, LOGP 18.33) between the markers Kukri_c27309_590 (48.57 cM) and BS00064538_51 (56.64 cM), defining a maximum mapping interval of 31.81 Mb – 34.23 Mb between the two mapping bins as several markers map to the 56.64 cM bin. The mean founder effects of the QTL predict a significant acceleration of flowering time for Soissons, which is the only founder carrying the photoperiod insensitive *Ppd-D1a* allele (Bentley *et al.* 2013) and furthermore *Ppd-D1* maps within the QTL (33.95 Mb). This analysis of the

effect of *Ppd-D1a* on flowering time validated MPWGAIM and our QTL mapping pipeline in MAGIC.

Synteny analysis between Chinese Spring and Jagger 1D

A conserved haplotype block between Cadenza and Jagger at the distal end of chromosome 1D was identified using the Crop Haplotypes web browser (Crop Haplotypes (crop-haplotypes.com) (Brinton *et al.* 2020). Physical locations of genes on the Chinese Spring 1D chromosome (IWGSCRefSeqv1.1) and Jagger 1D chromosome (PGSBv2.0) were mapped using the mapviewer v2.6.1 (https://10wheatgenomes.plantinformatics.io/mapview) and then confirmed manually using EnsemblPlants.

SNP mining and analysis

820k and 35k SNP array data was obtained from the CerealsDB website (Wilkinson *et al.* 2012) and the 1000Exome data from the 1000 Exomes project website (http://wheatgenomics.plantpath.ksu.edu/1000EC/). Mapping of 35k and 820k SNPs to the IWGSCv1.1 Ref sequence were obtained from EnsemblPlantsv51. SNPs for the Cadenza/Jagger haplotype (chr1D: 482.3Mb – end of chromosome 1D) were extracted and heterozygous calls set as missing. Distance matrices and phylogenetic trees were constructed using the R package “ape” (Paradis and Schliep 2019) 100 bootstrap permutations were run also using the R package “ape”.

To investigate the prevalence of the Ser674Gly SNP in a broad range of germplasm we analysed variation data from multiple sources including the 820k SNP genotyping array (Winfield *et al.* 2016), the wheat HapMap panel (Jordan *et al.* 2015), the 1000

wheat Exome project (He *et al.* 2019) and the 10+ Wheat Genome project (Walkowiak *et al.* 2020). We found that the Ser674Gly SNP was also present in the HapMap panel as chr1B_685645813 and within the 1000 Exome data as scaffold48561_337271.

Phylogenetic tree construction

ELF3-D1 orthologous groups were retrieved from public repositories. Coding sequences were aligned using the MCoffee aligner on default settings (https://pubmed.ncbi.nlm.nih.gov/16556910/). Maximum Likelihood (ML) Phylogenetic trees were build using CLC Genomics Workbench 21.0.3. The best substitution model was determined using the Model testing function before running Molecular Phylogenetic analysis by Maximum Likelihood method with 100 permutations for Bootstrap values. The *ELF3* gene from *Brachypodium distachyon* was used as an outgroup.

Quantitative Real-Time PCR

The *TtELF3*-WT and *Ttelf3*-null lines were sown and grown in two antiphased LED growth chambers (Conviron) under long day conditions (16h L: 8h D; 250 µmol m^{-2} s^{-1}, 20°C day: 16°C night). Sampling commenced 16 days post-sowing, the first true leaf was sampled every 3 hours for 96 hours. After the first 24 hours of sampling the cabinet was switched to constant light and temperature (250 µmol m^{-2} s^{-1} , 20°C). Total RNA was extracted from leaf samples using the KingFisher Flex purification system (Thermofisher scientific) in conjunction with the Maxwell® HT simplyRNA Kit (Promega). RNA concentration was determined using the Nanodrop ND-1000. DNA contamination was removed using the Arcticzyme HL-DNAse kit. RNA integrity was checked using the Fragment AnalyzerTM (AATI, USA) before cDNA was synthesised

from extracted RNA using the High-Capacity cDNA reverse transcription kit (Applied Biosystems). Three technical replicates of gene specific products were amplified in 10 µl reactions using Power SYBR Green Master mix on a CFX384 Touch Real-Time PCR detection system. Gene expression levels were determined relative to the expression of two housekeeping genes, *TtRP15* and *TtRPT5A,* that were selected using the GeNorm alogorithm (Vandesompele *et al.* 2002) (Table 5).

PCR of *ELF3-D1*

DNA extracted using the DNeasy plant mini extraction kit (Qiagen, UK). The presence of *ELF3-D1* was confirmed by PCR using the *TaELF3-D1* primers listed in Table 5. PCR was performed using the DreamTaq Green PCR kit (Thermo Scientific, UK) on a ProFlex PCR system (Thermo Scientific, UK). PCR reaction conditions were as follows: 3 minutes at 95ºC; 40 cycles of 30 s at 95ºC, 30 s at 68ºC, 90 s at 72ºC; 15 minutes at 72ºC.

Delayed chlorophyll fluorescence and prompt chlorophyll *a* fluorescence imaging

Leaf samples were taken from the upper half of the first true leaf of 16 day old seedlings (non-vernalised) and were cut into 3 mm by 3 mm pieces and placed on solid 0.8% (w/v) bactoagar, 0.5 x MS Vitamin medium (M3900, Sigma-Aldrich, UK) supplemented with 0.5 µM benzyl-aminopurine (BAP), poured in a black 96 well imaging plates (Greiner, UK). Delayed fluorescence (Gould *et al.* 2009) was measured for 60 s in an LB985 Nightshade (Berthold, UK) camera. Between measurements of

DF light was supplied from blue (470 nm) red (660 nm) and LED arrays at 100 µmol m^{-2} s^{-1} during the experiment. Temperature was maintained at 20ºC.

Chlorophyll *a* fluorescence and calculations of parameters were carried out using a CFimager (Technologica Ltd, Colchester, UK) and the image processing scripts provided by the manufacturer. Chlorophyll fluorescence images were captured using a Stingray F145B ASG camera (Allied Vision Technologies, UK) through an RG665 long pass filter to exclude blue light from the LEDs. When imaging under continuous light, leaf fragments were exposed to 40 minutes of 100 µmol m^{-2} s^{-1} of blue light followed by a saturating pulse of 6172 µmol m^{-2} s^{-1} blue light for 800 ms then 20 minutes of darkness (with non-actinic measuring light on) followed by a second saturating pulse of 6172 µmol m^{-2} s^{-1} for 800 ms.

Circadian measures of amplitude, phase, period and relative amplitude error were calculated using the FFT-NLLS method in Biodare2 (www.biodare2.ed.ac.uk) (Zielinski *et al.* 2014). Where necessary data was normalised to between -1 and 1 using the normalisation feature of Biodare2.

Direct contact leaf temperature measurements

Leaf surface temperature relative to background temperature was measured using an in-house built device and provides an alternative measure of circadian rhythms caused by circadian regulated changes in the stomatal aperture (Dakhiya and Green 2019). The temperature logger was validated by measuring circadian rhythms of “in-phase” and “anti-phase” wheat leaves where peak temperature, and therefore maximum closure, occurred during the subjective night (S12 Fig). Leaf temperature

measurements were taken from fully expanded flag leaf of 4-week-old plants under continuous light and temperature (200 µmol m^{-2} s^{-1}, 20°C) that were previously grown under long days (16h L: 8h D; 200 µmol m^{-2} s^{-1}, 20°C day: 15°C night) in a growth cabinet (Conviron, UK).

Wheat was grown in 10 cm pots. Circadian measurements of leaf temperature were taken when the pants were four-weeks old. Type-K thermocouples were attached to the leaf such the end of the thermocouple was pressing onto the surface of the fully expanded flag leaf. This was kept in position by positioning a paperclip onto the leaf and fixing the paperclip to a stake. The thermocouples were connected to an Arduino Mega using the Adafruit 1778, a 10 bit D-A converter and x20 amplifier giving a resolution of ± 0.1°C with a DS3231 RTC added to keep time, temperature was logged every 30 s. Background temperature was measured using unattached thermocouples. Leaf temperatures were averaged using a 60-point moving average, background temperature was then subtracted from leaf temperature to give leaf temperature relative to background.

Bibliography

Aguilar, M. and Prieto, P., 2020. Sequence analysis of wheat subtelomeres reveals a high polymorphism among homoeologous chromosomes. *The Plant Genome*, 13 (3), e20065.

Alvarez, M.A., Tranquilli, G., Lewis, S., Kippes, N., and Dubcovsky, J., 2016. Genetic and physical mapping of the earliness *per se* locus *Eps-A^{m}1* in *Triticum monococcum* identifies *EARLY FLOWERING 3* (*ELF3*) as a candidate gene. *Functional & Integrative Genomics*, 16 (4), 365–82.

Beales, J., Turner, A., Griffiths, S., Snape, J.W., and Laurie, D.A., 2007. A *Pseudo-Response Regulator* is misexpressed in the photoperiod insensitive *Ppd-D1a* mutant of wheat (*Triticum aestivum L.*). *Theoretical and Applied Genetics*, 115 (5), 721–733.

Bentley, A.R., Horsnell, R., Werner, C.P., Turner, A.S., Rose, G.A., Bedard, C., Howell, P., Wilhelm, E.P., Mackay, I.J., Howells, R.M., Greenland, A., Laurie, D.A., and Gosman, N., 2013. Short, natural, and extended photoperiod response in BC2F4 lines of bread wheat with different *Photoperiod-1* (*Ppd-1*) alleles. *Journal of Experimental Botany*, 64 (7), 1783–1793.

Boden, S.A., Weiss, D., Ross, J.J., Davies, N.W., Trevaskis, B., Chandler, P.M., and Swain, S.M., 2014. *EARLY FLOWERING3* Regulates Flowering in Spring Barley by Mediating Gibberellin Production and *FLOWERING LOCUS T* Expression. *The Plant Cell*, 26 (4), 1557–1569.

Brinton, J., Ramirez-Gonzalez, R.H., Simmonds, J., Wingen, L., Orford, S., Griffiths, S., Haberer, G., Spannagl, M., Walkowiak, S., Pozniak, C., and Uauy, C., 2020. A haplotype-led approach to increase the precision of wheat breeding. *Communications Biology*, 3 (1), 1–11.

Calixto, C.P.G., Waugh, R., and Brown, J.W.S., 2015. Evolutionary Relationships Among Barley and Arabidopsis Core Circadian Clock and Clock-Associated Genes. *Journal of Molecular Evolution*, 80 (2), 108–119.

Camargo, A. V., Mott, R., Gardner, K.A., Mackay, I.J., Corke, F., Doonan, J.H., Kim, J.T., and Bentley, A.R., 2016. Determining Phenological Patterns Associated with the Onset of Senescence in a Wheat MAGIC Mapping Population. *Frontiers in Plant Science*, 7, 1540.

Campoli, C., Pankin, A., Drosse, B., Casao, C.M., Davis, S.J., and Von Korff, M., 2013. *HvLUX1* is a candidate gene underlying the *early maturity 10* locus in barley: Phylogeny, diversity, and interactions with the circadian clock and photoperiodic pathways. *New Phytologist*, 199 (4), 1045–1059.

Clavijo, B.J., Venturini, L., Schudoma, C., Accinelli, G.G., Kaithakottil, G., Wright, J., Borrill, P., Kettleborough, G., Heavens, D., Chapman, H., Lipscombe, J., Barker, T., Lu, F.H., McKenzie, N., Raats, D., Ramirez-Gonzalez, R.H., Coince, A., Peel, N., Percival-Alwyn, L., Duncan, O., Trösch, J., Yu, G., Bolser, D.M., Namaati, G., Kerhornou, A., Spannagl, M., Gundlach, H., Haberer, G., Davey, R.P., Fosker, C., Di Palma, F., Phillips, A.L., Millar, A.H., Kersey, P.J., Uauy, C., Krasileva, K. V., Swarbreck, D., Bevan, M.W., and Clark, M.D., 2017. An improved assembly and annotation of the allohexaploid wheat genome identifies complete families of agronomic genes and provides genomic evidence for chromosomal translocations. *Genome Research*, 27 (5), 885–896.

Cockram, J., Jones, H., Leigh, F.J., O'Sullivan, D., Powell, W., Laurie, D.A., and Greenland, A.J., 2007. Control of flowering time in temperate cereals: genes, domestication, and sustainable productivity. *Journal of Experimental Botany*, 58 (6), 1231–1244.

Dakhiya, Y. and Green, R.M., 2019. Thermal imaging as a non-invasive technique for analyzing circadian rhythms in plants. *New Phytologist*, 224, 1685–1696.

Dakhiya, Y., Hussien, D., Fridman, E., Kiflawi, M., and Green, R., 2017. Correlations between Circadian Rhythms and Growth in Challenging Environments. *Plant Physiology*, 173 (3), 1724–1734.

Dixon, L.E., Knox, K., Kozma-Bognar, L., Southern, M.M., Pokhilko, A., and Millar, A.J., 2011. Temporal repression of core circadian genes is mediated through *EARLY FLOWERING 3* in Arabidopsis. *Current Biology*, 21 (2), 120–125.

Dodd, A.N., Salathia, N., Hall, A., Kévei, E., Tóth, R., Nagy, F., Hibberd, J.M., Millar, A.J., and Webb, A. a R., 2005. Plant circadian clocks increase photosynthesis, growth, survival, and competitive advantage. *Science (New York, N.Y.)*, 309 (5734), 630–633.

Ezer, D., Jung, J.H., Lan, H., Biswas, S., Gregoire, L., Box, M.S., Charoensawan, V., Cortijo, S., Lai, X., Stöckle, D., Zubieta, C., Jaeger, K.E., and Wigge, P.A., 2017. The evening complex coordinates environmental and endogenous signals in Arabidopsis. *Nature Plants*, 3 (7).

Faricelli, M.E., Valárik, M., and Dubcovsky, J., 2010. Control of flowering time and spike development in cereals: The *earliness per se Eps-1* region in wheat, rice, and *Brachypodium*. *Functional and Integrative Genomics*, 10 (2), 293–306.

Faure, S., Turner, a. S., Gruszka, D., Christodoulou, V., Davis, S.J., von Korff, M., and Laurie, D. a., 2012. Mutation at the circadian clock gene *EARLY MATURITY 8* adapts domesticated barley (*Hordeum vulgare*) to short growing seasons. *Proceedings of the National Academy of Sciences*, 109 (21), 8328–8333.

Gardner, K.A., Wittern, L.M., and Mackay, I.J., 2016. A highly recombined, high-

density, eight-founder wheat MAGIC map reveals extensive segregation distortion and genomic locations of introgression segments. *Plant Biotechnology Journal*, 14 (6), 1406–1417.

Gawronski, P., Ariyadasa, R., Himmelbach, A., Poursarebani, N., Kilian, B., Stein, N., Steuernagel, B., Hensel, G., Kumlehn, J., Sehgal, S.K., Gill, B.S., Gould, P., Hall, A., and Schnurbusch, T., 2014. A Distorted Circadian Clock Causes Early Flowering and Temperature-Dependent Variation in Spike Development in the *Eps-3^{A}m* Mutant of Einkorn Wheat. *Genetics*, 196 (4), 1253–1261.

Gendron, J.M., Pruneda-Paz, J.L., Doherty, C.J., Gross, A.M., Kang, S.E., and Kay, S.A., 2012. Arabidopsis circadian clock protein, TOC1, is a DNA-binding transcription factor. *Proceedings of the National Academy of Sciences*, 109 (8), 3167–3172.

Gerland, P., Raftery, A.E., Sevcikova, H., Li, N., Gu, D., Spoorenberg, T., Alkema, L., Fosdick, B.K., Chunn, J., Lalic, N., Bay, G., Buettner, T., Heilig, G.K., and Wilmoth, J., 2014. World population stabilization unlikely this century. *Science*, 346 (6206), 234–237.

Gilmour, A.R., Cullis, B.R., and Verbyla, A.P., 1997. Accounting for Natural and Extraneous Variation in the Analysis of Field Experiments. *Journal of Agricultural, Biological, and Environmental Statistics*, 2 (3), 269–293.

Gould, P.D., Diaz, P., Hogben, C., Kusakina, J., Salem, R., Hartwell, J., and Hall, A., 2009. Delayed fluorescence as a universal tool for the measurement of circadian rhythms in higher plants. *Plant Journal*, 58 (5), 893–901.

Griffiths, S., Simmonds, J., Leverington, M., Wang, Y., Fish, L., Sayers, L., Alibert, L., Orford, S., Wingen, L., Herry, L., Faure, S., Laurie, D., Bilham, L., and Snape, J., 2009. Meta-QTL analysis of the genetic control of ear emergence in

elite European winter wheat germplasm. *Theoretical and Applied Genetics*, 119 (3), 383–395.

Guo, W., Xin, M., Wang, Z., Yao, Y., Hu, Z., Song, W., Yu, K., Chen, Y., Wang, X., Guan, P., Appels, R., Peng, H., Ni, Z., and Sun, Q., 2020. Origin and adaptation to high altitude of Tibetan semi-wild wheat. *Nature Communications*, 11 (1), 1–12.

Hawkesford, M.J., Araus, J.L., Park, R., Calderini, D., Miralles, D., Shen, T., Zhang, J., and Parry, M. a. J., 2013. Prospects of Doubling Global Wheat Yields. *Food and Energy Security*, 2 (1), 34–48.

He, F., Pasam, R., Shi, F., Kant, S., Keeble-Gagnère, G., Kay, P., Forrest, K., Fritz, A., Hucl, P., Wiebe, K., Know, R., Cuthbert, R., Pozniak, C., Akhunova, A., Morrell, P.L., Davies, J.P., Webb, S.R., Spangenberg, G., Hayes, B., Daetwyler, H., Tibbits, J., Hayden, M., and Akhunov, E., 2019. Exome sequencing highlights the role of wild-relative introgression in shaping the adaptive landscape of the wheat genome. *Nature genetics*, 51 (5), 896–904.

Herrero, E., Kolmos, E., Bujdoso, N., Yuan, Y., Wang, M., Berns, M.C., Uhlworm, H., Coupland, G., Saini, R., Jaskolski, M., Webb, A., Goncalves, J., and Davis, S.J., 2012. EARLY FLOWERING4 Recruitment of EARLY FLOWERING3 in the Nucleus Sustains the *Arabidopsis* Circadian Clock. *the Plant Cell Online*, 24 (2), 428–443.

Hsu, P.Y. and Harmer, S.L., 2014. Wheels within wheels: The plant circadian system. *Trends in Plant Science*, 19 (4), 240–249.

Huang, B.E. and George, A.W., 2011. R/mpMap: A computational platform for the genetic analysis of multiparent recombinant inbred lines. *Bioinformatics*, 27 (5), 727–729.

Huang, H., Alvarez, S., Bindbeutel, R., Shen, Z., Naldrett, M.J., Evans, B.S., Briggs, S.P., Hicks, L.M., Kay, S.A., and Nusinow, D.A., 2016. Identification of evening complex associated proteins in *Arabidopsis* by affinity purification and mass spectrometry. *Molecular and Cellular Proteomics*, 15 (1), 201–217.

Huang, H., Gehan, M.A., Huss, S.E., Alvarez, S., Lizarraga, C., Gruebbling, E.L., Gierer, J., Naldrett, M.J., Bindbeutel, R.K., Evans, B.S., Mockler, T.C., and Nusinow, D.A., 2017. Cross-species complementation reveals conserved functions for *EARLY FLOWERING 3* between monocots and dicots. *Plant Direct*, 00, 1–14.

Huang, W., Perez-Garcia, P., Pokhilko, A., Millar, A.J., Antoshechkin, I., Riechmann, J.L., and Mas, P., 2012. Mapping the Core of the *Arabidopsis* Circadian Clock Defines the Network Structure of the Oscillator. *Science*, 336 (6077), 75–79.

Jordan, K.W., Wang, S., Lun, Y., Gardiner, L.-J., MacLachlan, R., Hucl, P., Wiebe, K., Wong, D., Forrest, K.L., Sharpe, A.G., Sidebottom, C.H., Hall, N., Toomajian, C., Close, T., Dubcovsky, J., Akhunova, A., Talbert, L., Bansal, U.K., Bariana, H.S., Hayden, M.J., Pozniak, C., Jeddeloh, J.A., Hall, A., and Akhunov, E., 2015. A haplotype map of allohexaploid wheat reveals distinct patterns of selection on homoeologous genomes. *Genome Biology*, 16 (1), 48.

Kolmos, E., Nowak, M., Werner, M., Fischer, K., Schwarz, G., Mathews, S., Schoof, H., Nagy, F., Bujnicki, J.M., and Davis, S.J., 2009. Integrating *ELF4* into the circadian system through combined structural and functional studies. *HFSP Journal*, 3 (5), 350–366.

Krasileva, K. V, Vasquez-gross, H.A., Howell, T., Bailey, P., Paraiso, F., and Clissold, L., 2017. Uncovering hidden variation in polyploid wheat. *PNAS*, E913–E921.

Langer, S.M., Longin, C.F.H., and Würschum, T., 2014. Flowering time control in European winter wheat. *Frontiers in Plant Science*, 5 (OCT), 1–11.

Lundqvist, U., 2014. Scandinavian mutation research in barley - a historical review. *Hereditas*, 151 (6), 123–131.

Mackay, I.J., Bansept-Basler, P., Bentley, A.R., Cockram, J., Gosman, N., Greenland, A.J., Horsnell, R., Howells, R., O'Sullivan, D.M., Rose, G.A., and Howell, P.J., 2014. An eight-parent multiparent advanced generation inter-cross population for winter-sown wheat: Creation, properties, and validation. *G3: Genes, Genomes, Genetics*, 4 (9), 1603–1610.

Matsubara, K., Ogiso-Tanaka, E., Hori, K., Ebana, K., Ando, T., and Yano, M., 2012. Natural variation in *Hd17*, a homolog of arabidopsis *ELF3* that is involved in rice photoperiodic flowering. *Plant and Cell Physiology*, 53 (4), 709–716.

McClung, C., 2019. The Plant Circadian Oscillator. *Biology*, 8 (1), 14.

Michael, T.P., Mockler, T.C., Breton, G., McEntee, C., Byer, A., Trout, J.D., Hazen, S.P., Shen, R., Priest, H.D., Sullivan, C.M., Givan, S.A., Yanovsky, M., Hong, F., Kay, S.A., and Chory, J., 2008. Network discovery pipeline elucidates conserved time-of-day-specific cis-regulatory modules. *PLoS Genetics*, 4 (2), 14.

Mizuno, N., Kinoshita, M., Kinoshita, S., Nishida, H., Fujita, M., Kato, K., Murai, K., and Nasuda, S., 2016. Loss-of-function mutations in three homoeologous *PHYTOCLOCK 1* genes in common wheat are associated with the extra-early flowering phenotype. *PLoS ONE*, 11 (10), 1–19.

Mizuno, N., Nitta, M., Sato, K., and Nasuda, S., 2012. A wheat homologue of *PHYTOCLOCK 1* is a candidate gene conferring the early heading phenotype to einkorn wheat. *Genes & genetic systems*, 87 (6), 357–67.

Nagel, D.H. and Kay, S.A., 2012. Complexity in the wiring and regulation of plant

circadian networks. *Current Biology*, 22 (16), 648–657.

Nusinow, D.A., Helfer, A., Hamilton, E.E., King, J.J., Imaizumi, T., Schultz, T.F., Farré, E.M., and Kay, S.A., 2011. The ELF4–ELF3–LUX complex links the circadian clock to diurnal control of hypocotyl growth. *Nature*, 475 (7356), 398–402.

Ochagavía, H., Prieto, P., Zikhali, M., Griffiths, S., and Slafer, G.A., 2019. Earliness Per Se by Temperature Interaction on Wheat Development. *Scientific Reports*, 9 (1), 2584.

Paradis, E. and Schliep, K., 2019. ape 5.0: an environment for modern phylogenetics and evolutionary analyses in R. *Bioinformatics*, 35 (3), 526–528.

Przewieslik-Allen, A.M., Wilkinson, P.A., Burridge, A.J., Winfield, M.O., Dai, X., Beaumont, M., King, J., Yang, C., Griffiths, S., Wingen, L.U., Horsnell, R., Bentley, A.R., Shewry, P., Barker, G.L.A., and Edwards, K.J., 2021. The role of gene flow and chromosomal instability in shaping the bread wheat genome. *Nature Plants*, 7 (2), 172–183.

Scutari, M., Howell, P., Balding, D.J., and Mackay, I., 2014. Multiple Quantitative Trait Analysis Using Bayesian Networks. *Genetics*, 198 (1), 129–137.

Shah, R., 2013. mpMapinteractive: Interactive components for package mpMap. R package version 0.2.

Shaw, L.M., Turner, A.S., and Laurie, D.A., 2012. The impact of photoperiod insensitive *Ppd-1a* mutations on the photoperiod pathway across the three genomes of hexaploid wheat (*Triticum aestivum*). *The Plant Journal*, 71 (1), 71–84.

Steed, G., Cano-Ramirez, D.L., Hannah, M.A., and Webb, A.A., 2021. Chronoculture, harnessing the circadian clock to improve crop yield and

sustainability. *Science*, 372 (April).

Sun, H., Zhang, W., Wu, Y., Gao, L., Cui, F., Zhao, C., Guo, Z., and Jia, J., 2020. The Circadian Clock Gene, *TaPRR1*, Is Associated With Yield-Related Traits in Wheat (*Triticum aestivum L.*). *Frontiers in Plant Science*, 11, 285.

Sun, L., Yang, W., Li, Y., Shan, Q., Ye, X., Wang, D., Yu, K., Lu, W., Xin, P., Pei, Z., Guo, X., Liu, D., Sun, J., Zhan, K., Chu, J., and Zhang, A., 2019. A wheat dominant dwarfing line with *Rht12* , which reduces stem cell length and affects gibberellic acid synthesis, is a 5AL terminal deletion line. *The Plant Journal*, 97 (5), 887–900.

Turner, A.S., Faure, S., Zhang, Y., and Laurie, D.A., 2013. The effect of day-neutral mutations in barley and wheat on the interaction between photoperiod and vernalization. *Theoretical and Applied Genetics*, 126 (9), 2267–2277.

Vandesompele, J., De Preter, K., Pattyn, F., Poppe, B., Van Roy, N., De Paepe, A., and Speleman, F., 2002. Accurate normalization of real-time quantitative RT-PCR data by geometric averaging of multiple internal control genes. *Genome biology*, 3 (7), RESEARCH0034.

Verbyla, A.P., George, A.W., Cavanagh, C.R., and Verbyla, K.L., 2014. Whole-genome QTL analysis for MAGIC. *Theoretical and Applied Genetics*, 127 (8), 1753–1770.

Walkowiak, S., Gao, L., Monat, C., Haberer, G., Kassa, M.T., Brinton, J., Ramirez-Gonzalez, R.H., Kolodziej, M.C., Delorean, E., Thambugala, D., Klymiuk, V., Byrns, B., Gundlach, H., Bandi, V., Siri, J.N., Nilsen, K., Aquino, C., Himmelbach, A., Copetti, D., Ban, T., Venturini, L., Bevan, M., Clavijo, B., Koo, D.H., Ens, J., Wiebe, K., N'Diaye, A., Fritz, A.K., Gutwin, C., Fiebig, A., Fosker, C., Fu, B.X., Accinelli, G.G., Gardner, K.A., Fradgley, N., Gutierrez-Gonzalez, J.,

Halstead-Nussloch, G., Hatakeyama, M., Koh, C.S., Deek, J., Costamagna, A.C., Fobert, P., Heavens, D., Kanamori, H., Kawaura, K., Kobayashi, F., Krasileva, K., Kuo, T., McKenzie, N., Murata, K., Nabeka, Y., Paape, T., Padmarasu, S., Percival-Alwyn, L., Kagale, S., Scholz, U., Sese, J., Juliana, P., Singh, R., Shimizu-Inatsugi, R., Swarbreck, D., Cockram, J., Budak, H., Tameshige, T., Tanaka, T., Tsuji, H., Wright, J., Wu, J., Steuernagel, B., Small, I., Cloutier, S., Keeble-Gagnère, G., Muehlbauer, G., Tibbets, J., Nasuda, S., Melonek, J., Hucl, P.J., Sharpe, A.G., Clark, M., Legg, E., Bharti, A., Langridge, P., Hall, A., Uauy, C., Mascher, M., Krattinger, S.G., Handa, H., Shimizu, K.K., Distelfeld, A., Chalmers, K., Keller, B., Mayer, K.F.X., Poland, J., Stein, N., McCartney, C.A., Spannagl, M., Wicker, T., and Pozniak, C.J., 2020. Multiple wheat genomes reveal global variation in modern breeding. *Nature*, 588 (7837), 277–283.

Wang, J., Wen, W., Hanif, M., Xia, X., Wang, H., Liu, S., Liu, J., Yang, L., Cao, S., and He, Z., 2016. *TaELF3-1DL*, a homolog of *ELF3*, is associated with heading date in bread wheat. *Molecular Breeding*, 36 (12), 1–9.

Wang, Z.Y., Kenigsbuch, D., Sun, L., Harel, E., Ong, M.S., and Tobin, E.M., 1997. A Myb-related transcription factor is involved in the phytochrome regulation of an Arabidopsis Lhcb gene. *The Plant Cell*, 9 (4), 491–507.

Weller, J.L., Liew, L.C., Hecht, V.F.G., Rajandran, V., Laurie, R.E., Ridge, S., Wenden, B., Schoor, J.K.V., Jaminon, O., Blassiau, C., Dalmais, M., Rameau, C., Bendahmane, A., Macknight, R.C., and Lejeune-Hénaut, I., 2012. A conserved molecular basis for photoperiod adaptation in two temperate legumes. *Proceedings of the National Academy of Sciences of the United States of America*, 109 (51), 21158–21163.

Wilkinson, P.A., Winfield, M.O., Barker, G.L.A., Allen, A.M., Burridge, A., Coghill, J.A., and Edwards, K.J., 2012. CerealsDB 2.0: an integrated resource for plant breeders and scientists. *BMC Bioinformatics*, 13 (1), 219.

Winfield, M.O., Allen, A.M., Burridge, A.J., Barker, G.L.A., Benbow, H.R., Wilkinson, P.A., Coghill, J., Waterfall, C., Davassi, A., Scopes, G., Pirani, A., Webster, T., Brew, F., Bloor, C., King, J., West, C., Griffiths, S., King, I., Bentley, A.R., and Edwards, K.J., 2016. High-density SNP genotyping array for hexaploid wheat and its secondary and tertiary gene pool. *Plant Biotechnology Journal*, 14 (5), 1195–1206.

Yao, W., Li, G., Yu, Y., and Ouyang, Y., 2018. funRiceGenes dataset for comprehensive understanding and application of rice functional genes. *GigaScience*, 7 (1), 1–9.

Zadoks, J.C., Chang, T.T., and Konzak, C.F., 1974. A decimal code for the growth stages of cereals. *Weed Research*, 14 (6), 415–421.

Zakhrabekova, S., Gough, S.P., Braumann, I., Muller, A.H., Lundqvist, J., Ahmann, K., Dockter, C., Matyszczak, I., Kurowska, M., Druka, A., Waugh, R., Graner, A., Stein, N., Steuernagel, B., Lundqvist, U., and Hansson, M., 2012. Induced mutations in circadian clock regulator *Mat-a* facilitated short-season adaptation and range extension in cultivated barley. *Proceedings of the National Academy of Sciences*, 109 (11), 4326–4331.

Zhai, H., Jiang, C., Zhao, Y., Yang, S., Li, Y., Yan, K., Wu, S., Luo, B., Du, Y., Jin, H., Liu, X., Zhang, Y., Lu, F., Reynolds, M., Ou, X., Qiao, W., Jiang, Z., Peng, T., Gao, D., Hu, W., Wang, J., Gao, H., Yin, G., Zhang, K., Li, G., and Wang, D., 2021. Wheat heat tolerance is impaired by heightened deletions in the distal end of 4AL chromosomal arm. *Plant Biotechnology Journal*, 19 (5), 1038–1051.

Zhao, J., Huang, X., Ouyang, X., Chen, W., Du, A., and Zhu, L., 2012. *OsELF3-1* , an Ortholog of *Arabidopsis EARLY FLOWERING 3* , Regulates Rice Circadian Rhythm and Photoperiodic Flowering. *PLoS ONE*, 7 (8), 1–10.

Zielinski, T., Moore, A.M., Troup, E., Halliday, K.J., and Millar, A.J., 2014. Strengths and limitations of period estimation methods for circadian data. *PLoS ONE*, 9 (5).

Zikhali, M., Wingen, L.U., and Griffiths, S., 2016. Delimitation of the *Earliness per se D1* (*Eps-D1*) flowering gene to a subtelomeric chromosomal deletion in bread wheat (*Triticum aestivum*). *Journal of Experimental Botany*, 67 (1), 287–299.

Figures

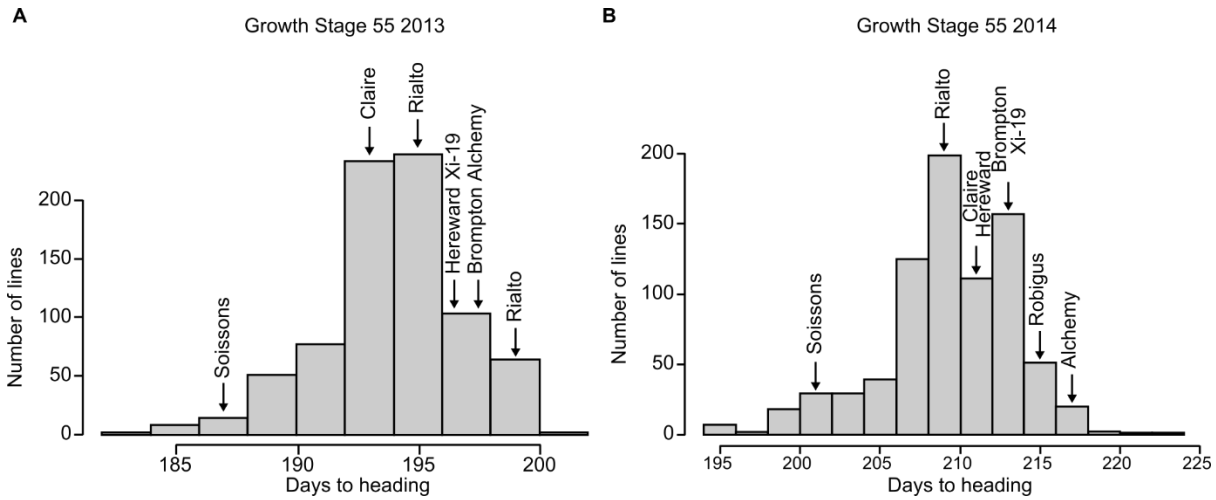

Fig 1. **Variation in time to reach GS55 across a UK wheat MAGIC population**.

Time in days for individual MAGIC RILs (recombinant inbred lines) to reach GS55 for the (A) 2012/2013 growing season and (B) 2013/2014 growing season. The number of days after sowing to reach GS55 for the eight MAGIC parents is indicated by arrows.

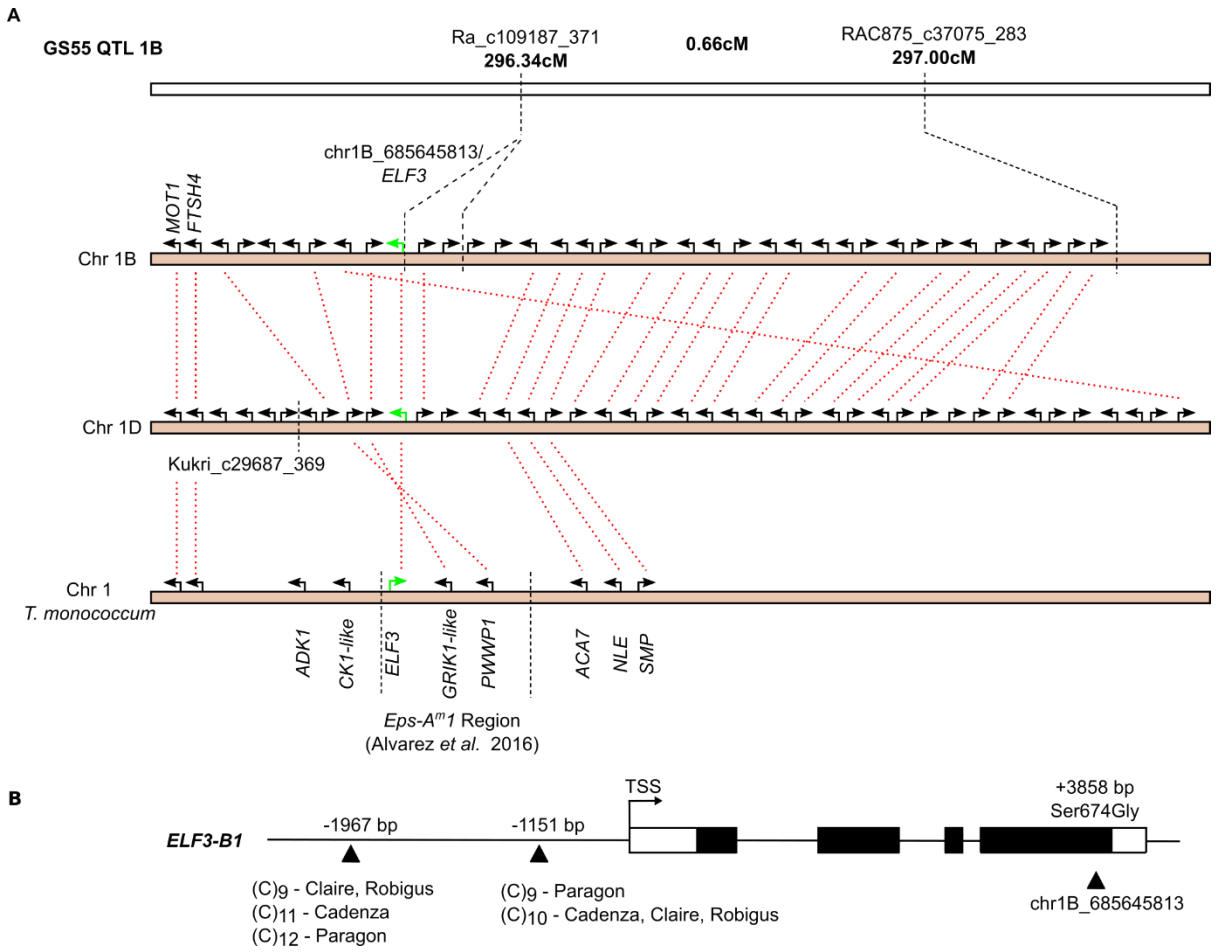

Fig 2. ***ELF3* is a candidate gene for *Eps-B1*.**

(A) Syntenic relationships of the *Eps-B1* QTL to the *Eps-D1* QTL and the *T. monococcum Eps-A^{m}1* QTL. *ELF3* highlighted in green. (B) *TaELF3-B1* gene model with exons represented by filled rectangles, UTR's as white rectangles. The two promoter cytosine repeat polymorphisms with location relative to the transcription start site (TSS) are indicated with the cytosine (C) repeat number for Claire, Robigus, Cadenza and Paragon. The Ser674Gly SNP is situated within exon 4 of *ELF3-B1.*

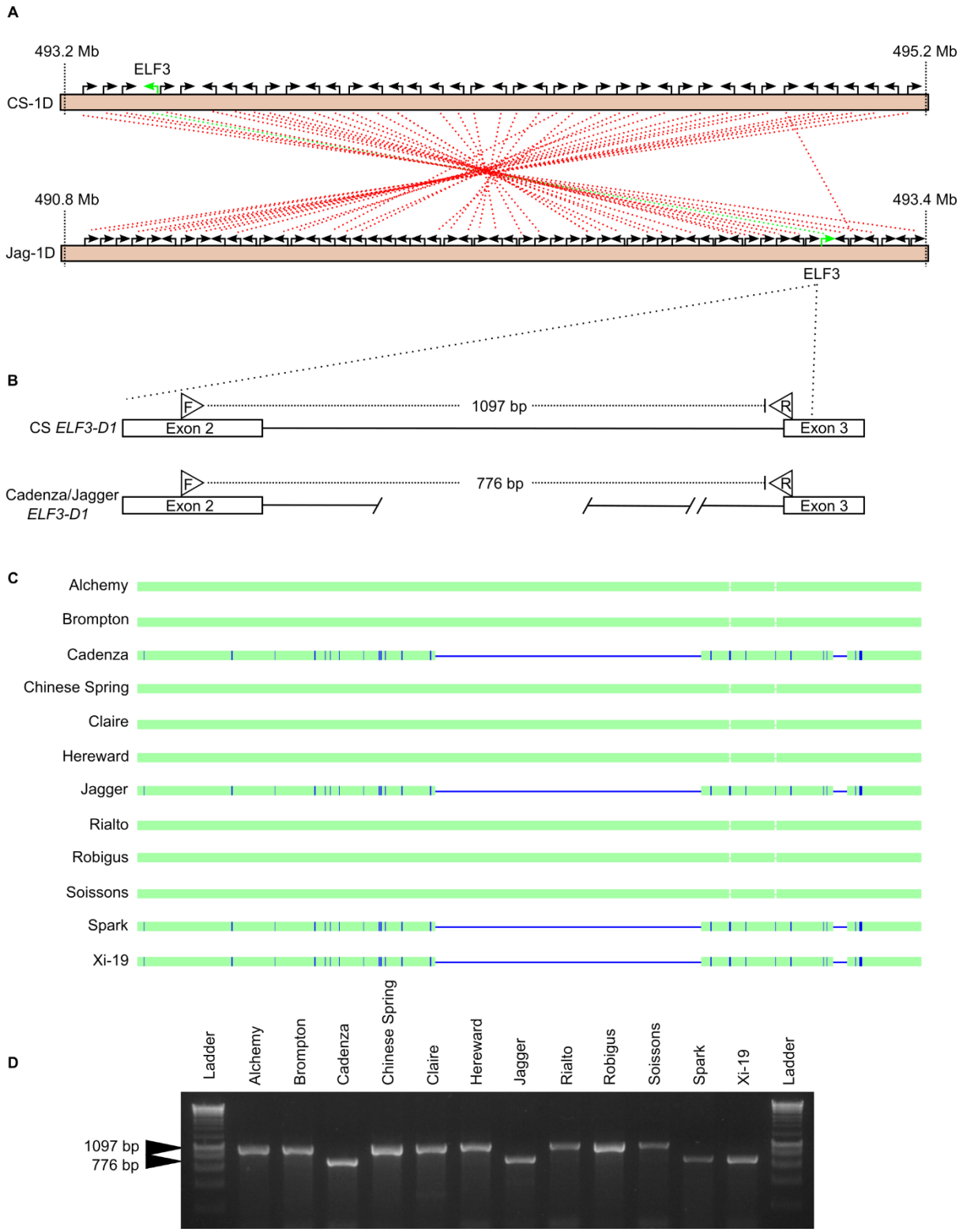

Fig 3. A subtelomeric chromosomal introgression and inversion containing *ELF3-D1* is likely to be the causal polymorphism underlying the *Eps-D1* QTL.

(A) Syntenic relationships between the distal end of Chinese Spring (CS) 1D chromosome (IWGSCv1.1) and Jagger (Jag) 1D (PGSBv2.0), *TaELF3-D1* highlighted in green, each black arrow corresponds to a gene in the forward (pointing right) or reverse (pointing left) strand. (B) the Cadenza/Jagger *ELF3-D1*

contains a deletion within intron 2 which is not present in CS, F and R refer to relative primer binding sites for PCR amplification shown in (C). (D) Agarose gel separation of PCR products from (C). A PCR product at 776bp is indicative of the presence of a subtelomeric chromosomal introgression and inversion.

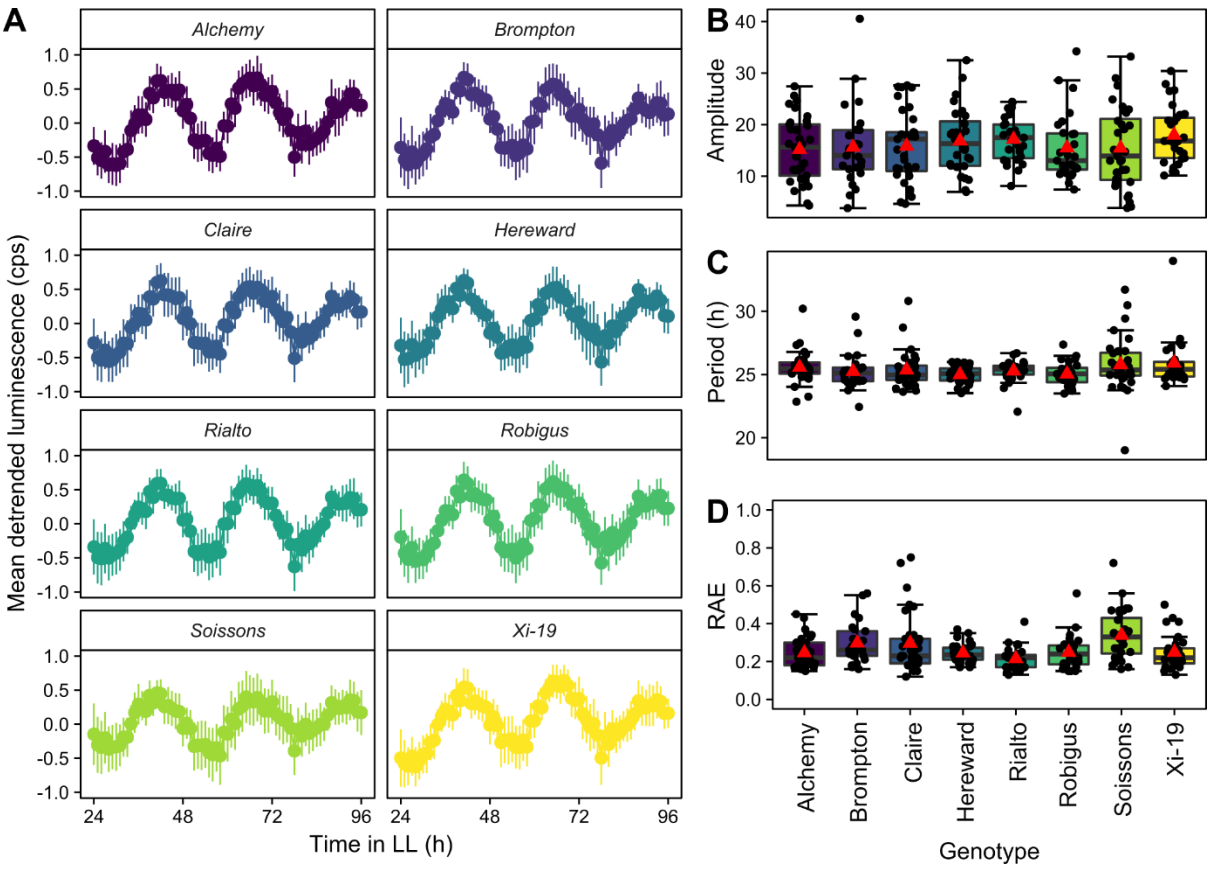

Fig 4. Circadian rhythms of delayed chlorophyll fluorescence in the MAGIC parents. (A) Mean DF luminescence in counts per second (cps) normalised to -1 to 1 using Biodare2 with error bars representing standard deviation (n = 27 - 33). Circadian amplitude (B), period (C) and RAE (D) calculated using FFT-NLLS (Biodare2). Upper and lower hinges represent the first and third quartiles (25th and 75th percentiles), the middle hinge represents the median value, red triangle represents mean value and black dots represent individual replicates.

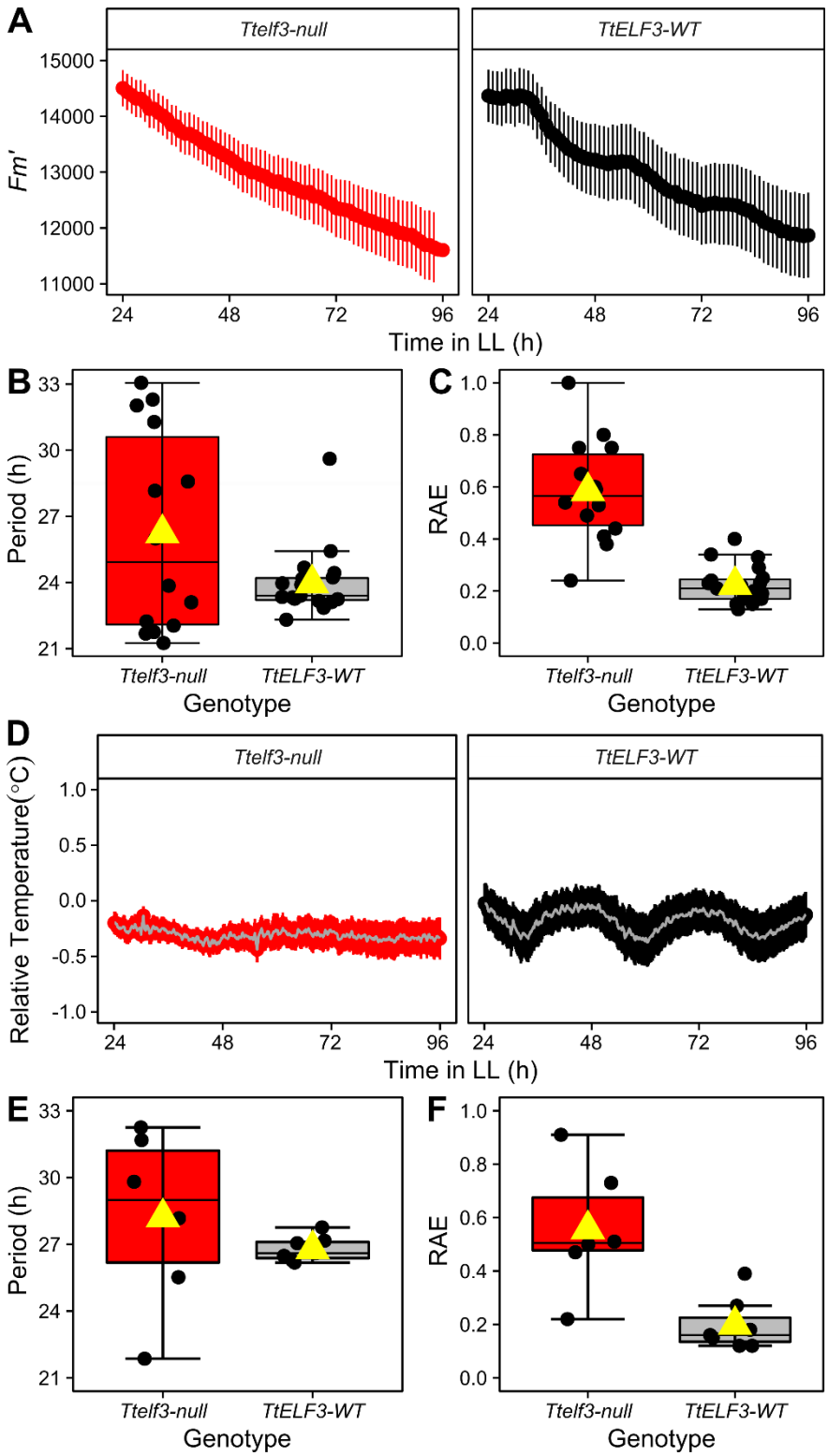

Fig 5. *Ttelf3*-null is arrhythmic in continuous light.

(A) Mean *Fm'* of *Ttelf3*-null (red) and *TtELF3-WT* (black) in LL (n = 24) (B) Mean period length (hours) and (C) RAE values for plot (A). Upper and lower hinges represent the first and third quartiles (25th and 75th percentiles), the middle hinge represents the median value, yellow triangle represents mean value and black dots represent individual replicates. (D) Mean leaf surface temperature relative to

background and normalised to the mean in LL and constant environmental temperature (20°C) for *Ttelf3-null* (red) *TtELF3-WT* (black) and *Ttelf3-null* (red) (n = 7) (E) Mean period length and (F) RAE for plot (D). For clarity every 20th point plotted in (D). Error bars represent SEM.

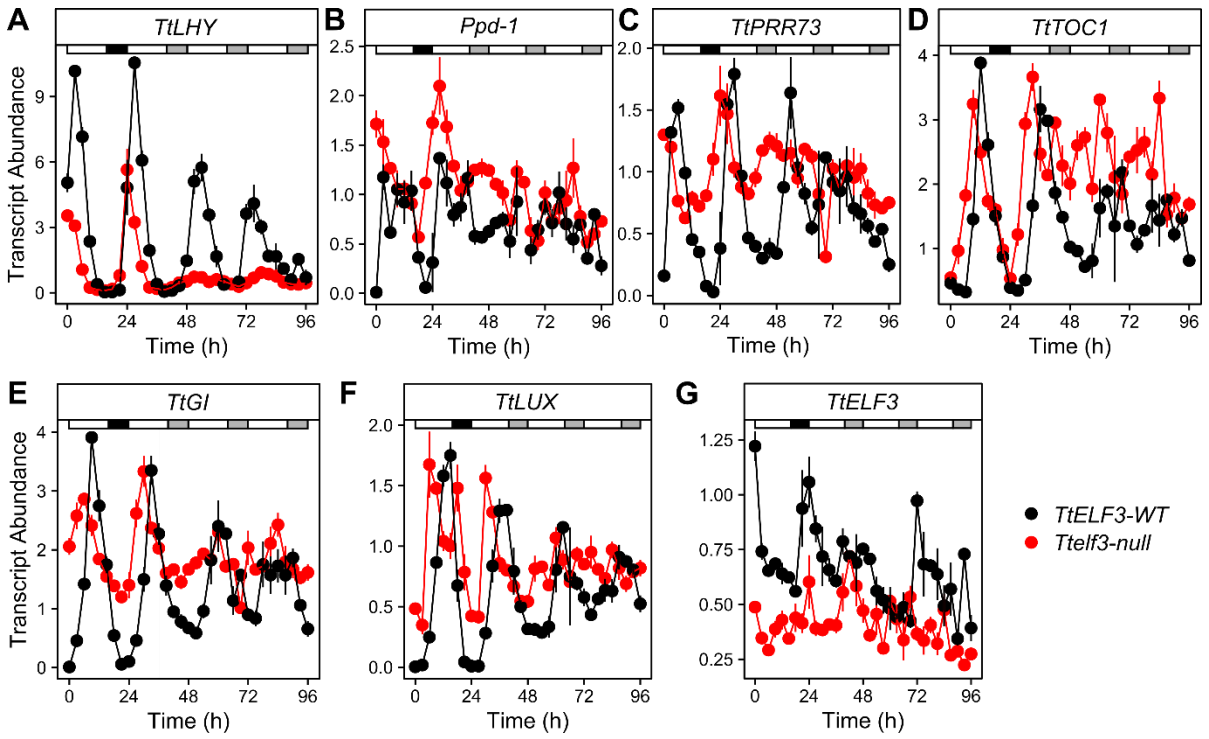

Fig 6. Abundance of wheat circadian clock transcripts in the *TtELF3-WT* and *ttelf3* lines in LD and LL.

(A-G) Mean abundance of circadian oscillator transcripts (n= 3 - 5) in *TtELF3*-WT (black) and *Ttelf3*-null (red) in a 24 h LD cycle in long day conditions (16 h light at 250 µmol m^{-2} s^{-1}, 20°C: 8 h dark 16°C, represented by vertical grey bar) followed by constant light and temperature (20°C) from time 24 to 96 h. Transcript abundance (ΔΔCq) is relative to *TtRP15* and *TtRPT5A* (A) *TtLHY,* (B) *Ppd-1,* (C) *TtPRR73,* (D) *TtTOC1,* (E) *TtGI,* (F) *TtLUX* and (G) *TtELF3* . White bar represents light, black bar represents darkness and grey bar represents subjective night.

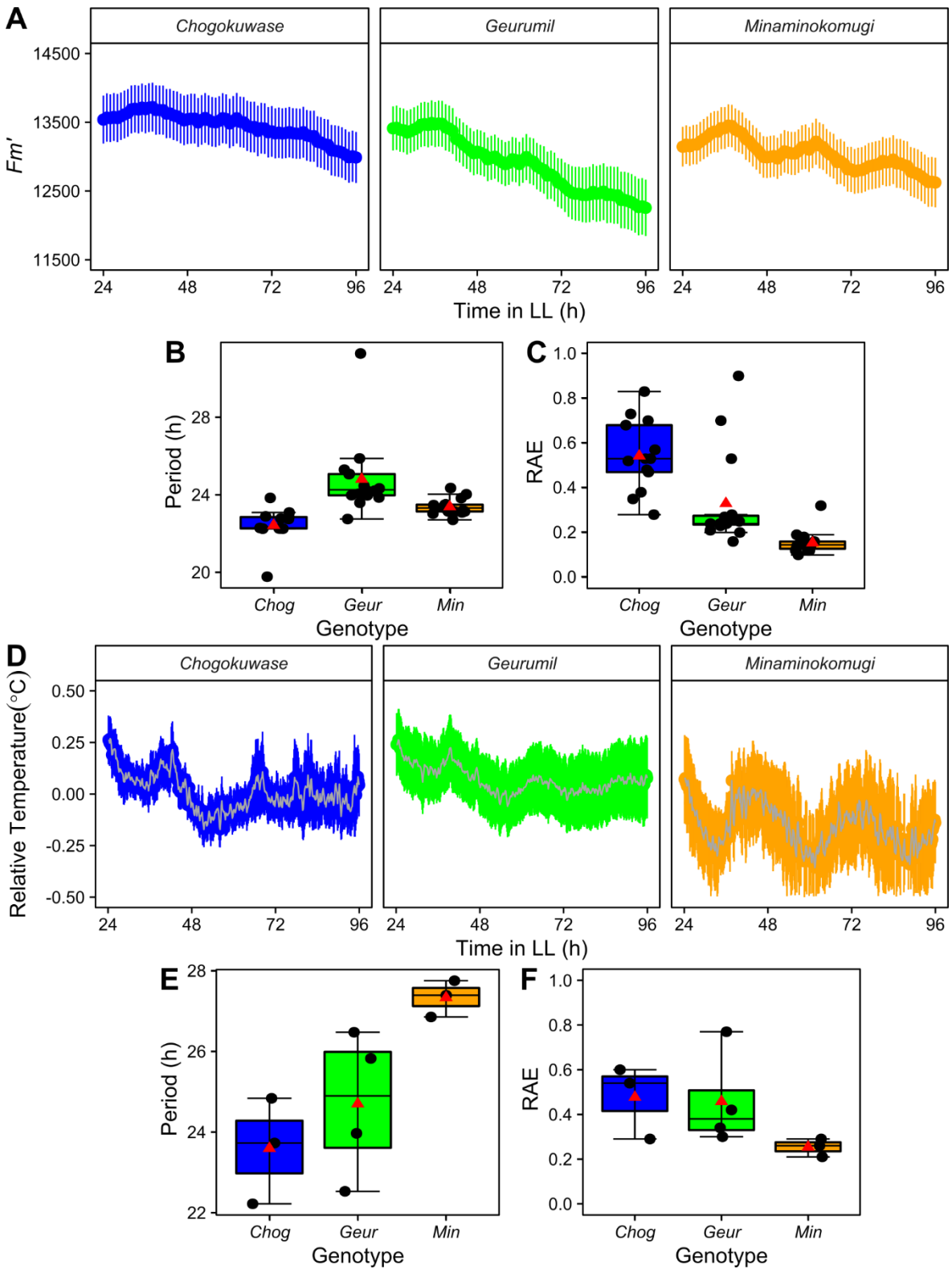

Fig 7. Functional *LUX* is required for maintenance of robust circadian oscillations under LL conditions in hexaploid wheat.

(A) Mean $F_{m'}$ for Chogokuwase (blue), Geurumil (green) and Minaminokomugi (orange) in LL (n = 16) (B) Mean period and (C) RAE for (A) calculated using FFT-NLLS (Biodare2). Upper and lower hinges

represent the first and third quartiles (25th and 75th percentiles), the middle hinge represents the median value, red triangle represents mean value and black dots represent individual replicates. (D) Mean Chogokuwase, Geurumil and Minaminokomugi leaf temperature relative to background in LL (n = 4). (E) mean period and (F) RAE for plot (D). Error bars are SEM, for (D) every 20th point plotted for clarity.

Table 1: **Summary of circadian clock associated QTLs and their mapping positions.** Output from univariate QTL model for the NIAB 2013 and 2014 GS55 data. Gene (Mb) refers to the BLAST hit starting coordinate of the gene's cDNA against the IWGSCRefSeqv1.1. Dist (cM) refers to the markers genetic mapping distance in centiMorgan. Dist (Mb) refers to the BLAST hit starting coordinate of the marker sequence against the IWGSCRefSeqv1.1 LOGP is –log10(p) which corresponds to the overall significance of the QTLs as a measure of its strength. % var is the percentage of genetic variance contributed by QTL. Further description of methodology and column headers can be found in (Verbyla et al. 2014).

Circadian clock gene	Gene (Mb)	Chr	L. Marker	dist (cM)	dist (Mb)	R. Marker	dist (cM)	dist (Mb)	Year	LOGP	% var
TaELF3	685,646,575	1B	Ra_c109187_371	296.34	685,741,261	RAC875_c37075_283	297	687,715,336	2013	4.48	3.4
		1B	Ra_c109187_371	296.34	685,741,261	RAC875_c37075_284	297	687,715,336	2014	3.2	2
TaELF3	493,485,612	1D	Kukri_c29687_369	100.95	493,212,138	Kukri_rep_c69829_307	101.95	488,577,079	2014	2.32	4.1
Ppd-1	33,952,591	2D	Kukri_c27309_590	48.57	31,806,310	BS00064538_51	56.64	33,370,535	2013	20.04	17.2
		2D	Kukri_c27309_590	48.57	31,806,310	BS00064538_51	56.64	33,370,535	2014	43.92	30.2
TaZTL	625,638,942	7A	Kukri_c6676_172	207.62	610,934,248	Ku_c2990_1939	208.12	621,322,194	2013	2.87	2.6

Table 2. 2013 and 2014 GS55 QTL summary for the *eps-B1 locus*. Estimated parental haplotype effects on RIL BLUPs. Abbreviations as per (Verbyla *et al.* 2014): Dist (cM) refers to the markers genetic mapping distance in centiMorgans (cM). LOGP is –log10(p) and corresponds to the overall significance of the QTL as a measure of its strength. Founder Prob: probability QTL is from founder shown (p). Strength of associations can thus be reported at the overall or founder level. Size: Size of effect of each founder allele (days to GS55).

QTL	Year	Founder	Size	Founder Prob	% var	LOGP	KASP (chr1B:685645813)
Eps-B1	2013	Alchemy	-0.555	0.054	3.4	4.48	A:A
		Brompton	0.317	0.123			G:G
		Claire	-0.076	0.415			A;A
		Hereward	0.623	0.008			G:G
		Rialto	0.331	0.118			G:G
		Robigus	-0.102	0.376			A:A
		Soissons	-0.683	0.003			A:A
		Xi-19	0.053	0.426			G:G
Eps-B1	2014	Alchemy	-0.448	0.196	2	3.2	A:A
		Brompton	0.395	0.178			G:G
		Claire	-0.442	0.202			A:A
		Hereward	0.591	0.072			G:G
		Rialto	0.39	0.182			G:G
		Robigus	-0.313	0.264			A:A
		Soissons	-1.085	0.002			A:A
		Xi-19	0.453	0.15			G:G

Table 3. 2012 and 2014 GS55 QTL summary for the *eEps-D1 locus*. Estimated parental haplotype effects on RIL BLUPs. Abbreviations as per (Verbyla *et al.* 2014): Dist (cM) refers to the markers genetic mapping distance in centiMorgans (cM). LOGP is –log10(p) and corresponds to the overall significance of the QTL as a measure of its strength. Founder Prob: probability QTL is from founder shown (p). Strength of associations can thus be reported at the overall or founder level. Size: Size of effect of each founder allele (days to GS55).

QTL	Year	Founder	Size	Founder Prob	% var	LOGP	PCR (Figure 3D)
Eps-D1	2012	Alchemy	0.552	0.254	0.9	0.56	1097bp
		Brompton	0.105	0.446			1097bp
		Claire	-0.11	0.447			1097bp
		Hereward	0.021	0.49			1097bp
		Rialto	-0.044	0.477			1097bp
		Robigus	0.003	0.498			1097bp
		Soissons	0.734	0.134			1097bp
		Xi-19	-1.261	0.015			776bp
Eps-D1	2014	Alchemy	-0.058	0.472	4.1	2.32	1097bp
		Brompton	0.869	0.104			1097bp
		Claire	-1.412	0.051			1097bp
		Hereward	-0.582	0.252			1097bp
		Rialto	-0.071	0.457			1097bp
		Robigus	-0.265	0.38			1097bp
		Soissons	1.244	0.013			1097bp
		Xi-19	-0.79	0.053			776bp

Table 4: Wheat lines used in this study. GRU refers to the germplasm resource unit at the John Innes Centre, Norwich.

Species	Cultivar	Genotype	Reference
Ae. speltoides			GRU 2140023
T. aestivum	Alchemy		(Mackay *et al.* 2014)
T. aestivum	Brompton		(Mackay *et al.* 2014)
T. aestivum	Claire		(Mackay *et al.* 2014)
T. aestivum	Hereward		(Mackay *et al.* 2014)
T. aestivum	Rialto		(Mackay *et al.* 2014)
T. aestivum	Robigus		(Mackay *et al.* 2014)
T. aestivum	Soissons		(Mackay *et al.* 2014)
T. aestivum	Xi-19		(Mackay *et al.* 2014)
T. aestivum	Cadenza		GRU WBCDB0013-PG1
T. aestivum	Jagger		GRU PANG0006
T. aestivum	Spark		GRU WBCDB0052
T. aestivum	Chinese Spring		
T. aestivum	Chogokuwase		(Mizuno *et al.* 2016)
T. aestivum	Minaminokomugi		(Mizuno *et al.* 2016)
T. aestivum	Geurumil		(Mizuno *et al.* 2016)
T. aestivum	Axona		GRU W3580
T. aestivum	Cordiale		GRU W10003
T. aestivum	Maris Fundin		GRU W1357
T. aestivum	Tonic		GRU W3572
T. monococcum			GRU T1040057
T. sphaerococcum			GRU 1210007
T. timopheevii			GRU 116002
T. turgidum	Kronos	*Ttelf3*-null line	(Alvarez *et al.* 2016)
T. turgidum	Kronos	*TtELF3*-WT	(Alvarez *et al.* 2016)

Table 5: Primers used in this study

Gene	Sequence 5'-3'
TtCCA1	F: CCTGGAATTGGAGATGGAGA
	R: TGAGCATGGCTTCTGATTTG
TtELF3	F: TCTCCAGATGATGTTGTCGGT
	R: CTCGAACACTTGGACAGCAAA
TtGI	F: GGTAGGTGATAGACGGCACTT
	R: GTGCTACAGATGGGATGCTTG
TtLUX	F: ACAAGCGGTTCGTGGAGG
	R: CCTGCATCCGCTTGACGTA
TtPpd-1	F: CCTGTGGACTGTCGATCTCAA
	R: CAAGGGATGGCAGCGATAATG
TtPRR73	F: TCCCGAAGTTCCTCTCTTTCC
	R: AGCGGTAGTGGCAATGACA
TtTOC1	F: GGCATGGCACTTCATTCAGTT
	R: GCACATTCATACCAGCAGGAC
TtRP15	F: GCACACGTGCTTTGCAGATAAG
	R: GCCCTCAAGCTCAACCATAACT
TtRPT5A	F: GCTGGCTCGTTCAACTGATG
	R: GGACCAAGCGTTCTGATTACTC
TaELF3-D1	F: CAACGGCGCTTCTAATCTG
	R: AAACCCGCTGCTGACTGTATA

Supporting information

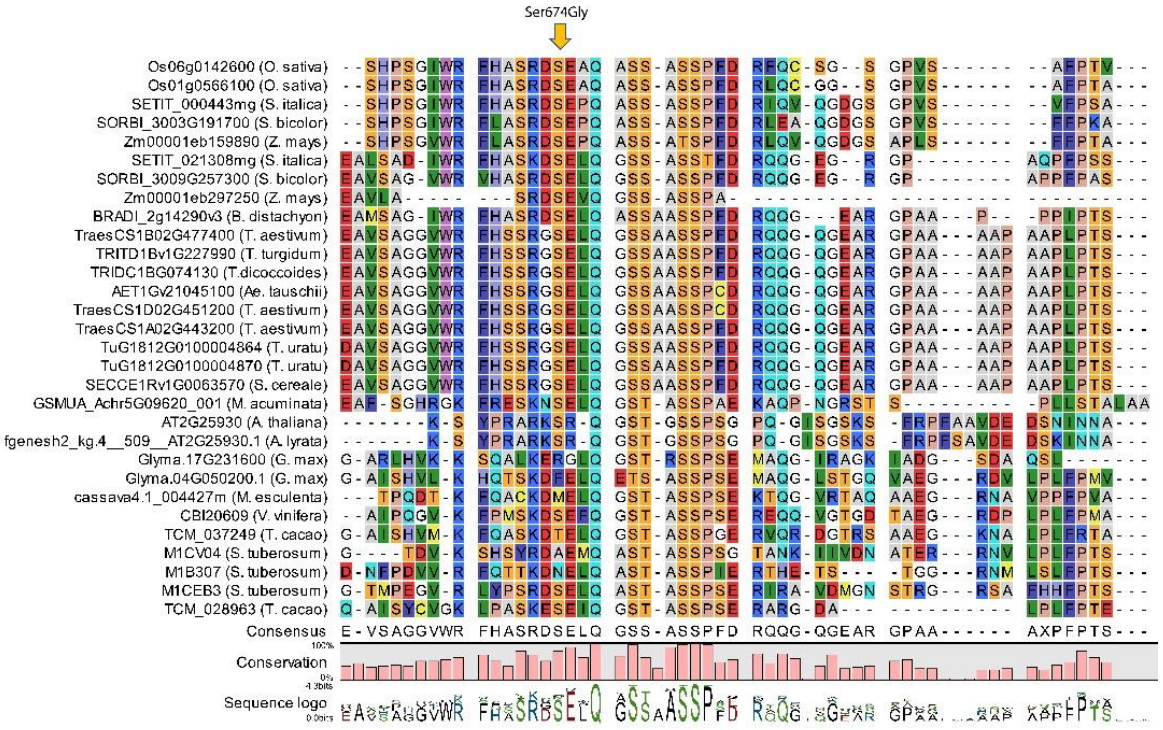

Figure S1 The Ser674 is highly conserved in monocots. MCoffee alignment visualised in CLC Genomics Workbench, Amino acids coloured based on RasMol colour scheme.

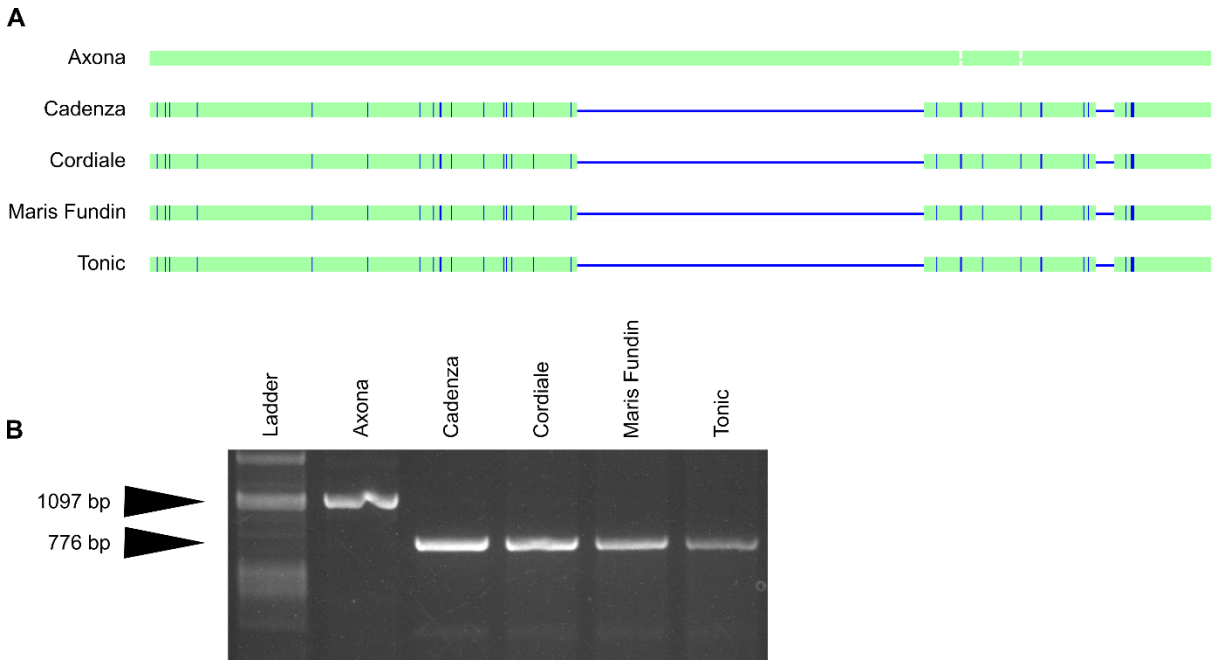

S2 Fig. The Cadenza/Jagger *ELF3-D1* intronic deletion is present within Cordiale, Maris Fundin and Tonic.
(A) Sequence alignment for PCR fragments between exon 2 and 3 of *ELF3-D1* (see Fig 3) and (B) Agarose gel separation of PCR products. A PCR product at 776bp is indicative of the presence of the introgressed and inverted region.

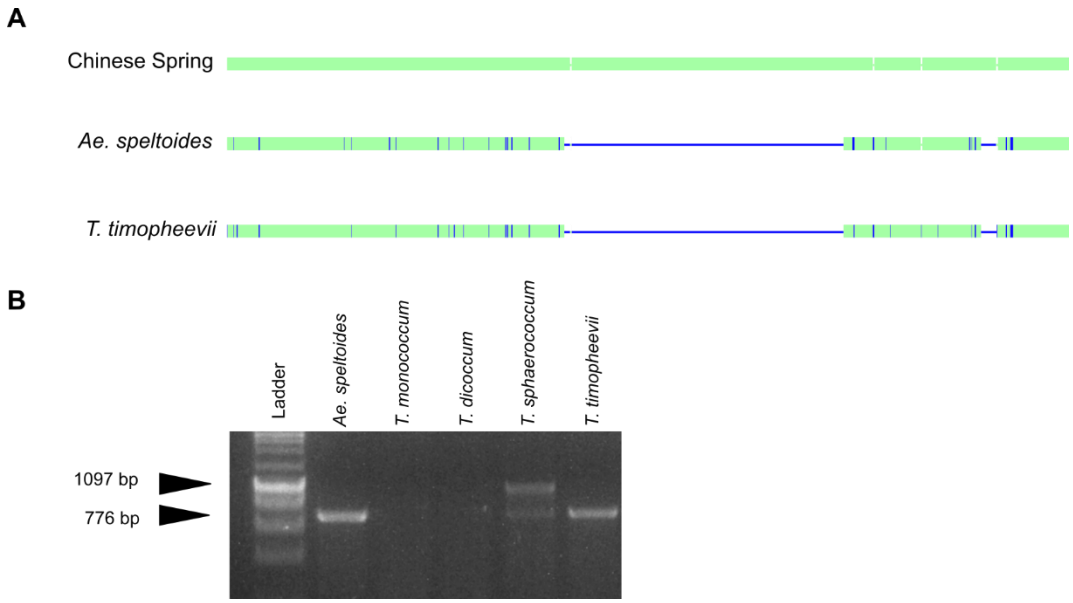

S3 Fig. The Cadenza/Jagger *ELF3-D1* intronic deletion is present within *Ae. speltoides* and *T. timopheevii.*

(A) Sequence alignment for PCR fragments between exon 2 and 3 of *ELF3-D1* (see Fig 3) and (B) Agarose gel separation of PCR products. A PCR product at 776bp is indicative of the presence of the introgressed and inverted region.

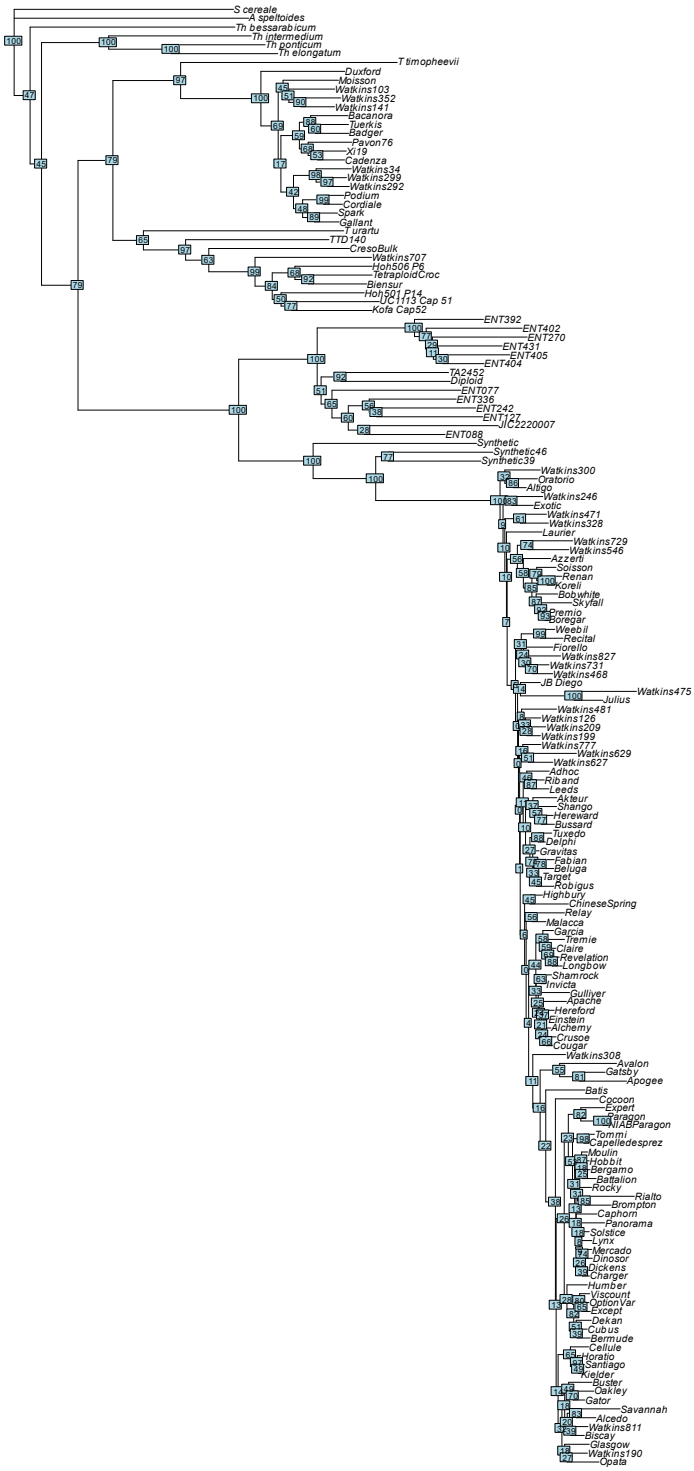

S4 Fig. Phylogeny of the 1D Jagger/ Cadenza shared haplotype using the 820k SNP dataset from CerealsDB.

Neighbour Joining Tree and bootstraps created from 820k SNPs using R package “ape”. All SNPs mapping to the CS coordinates (1D:482.83Mb until 1D end) of the shared Cadenza and Jagger haplotype were used. Heterozygotes were set as missing.

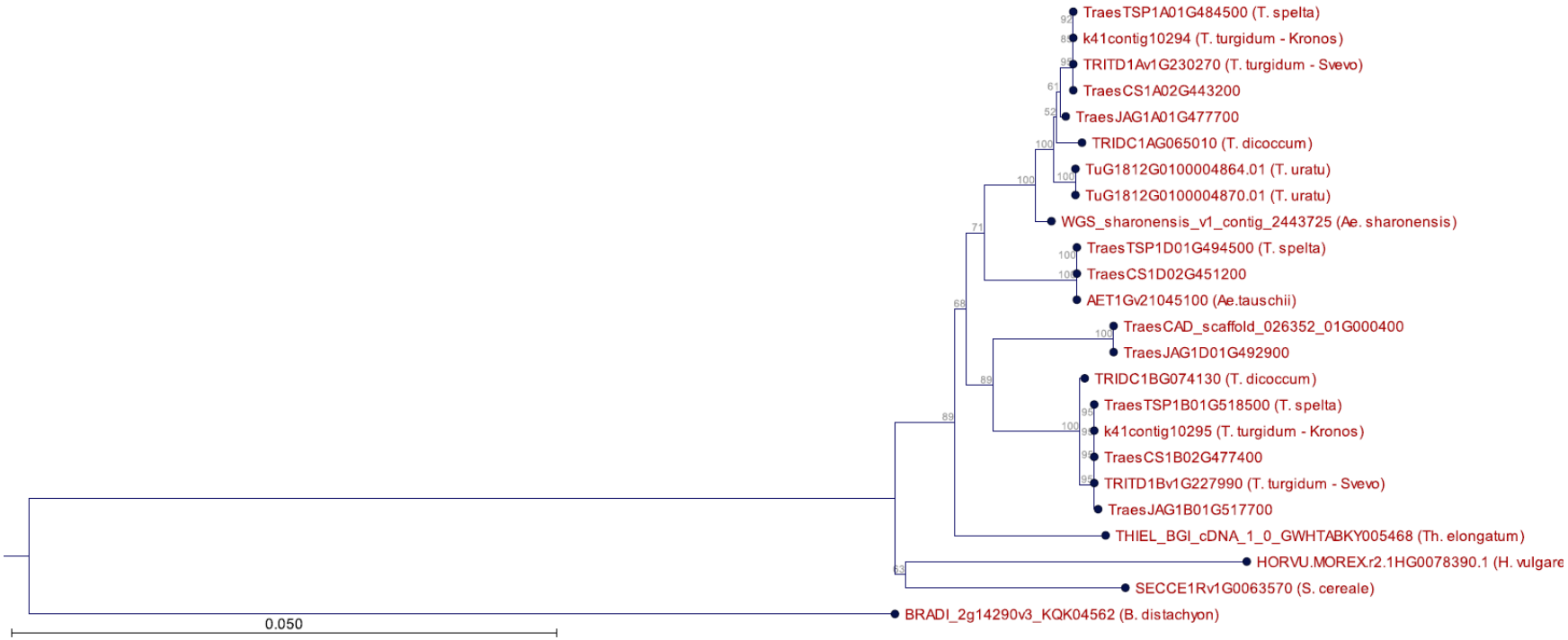

S5 Fig. Phylogeny of *ELF3-D1* gene.

Maximum Likelihood phylogeny based on T-coffee alignment of publicly available coding sequences.

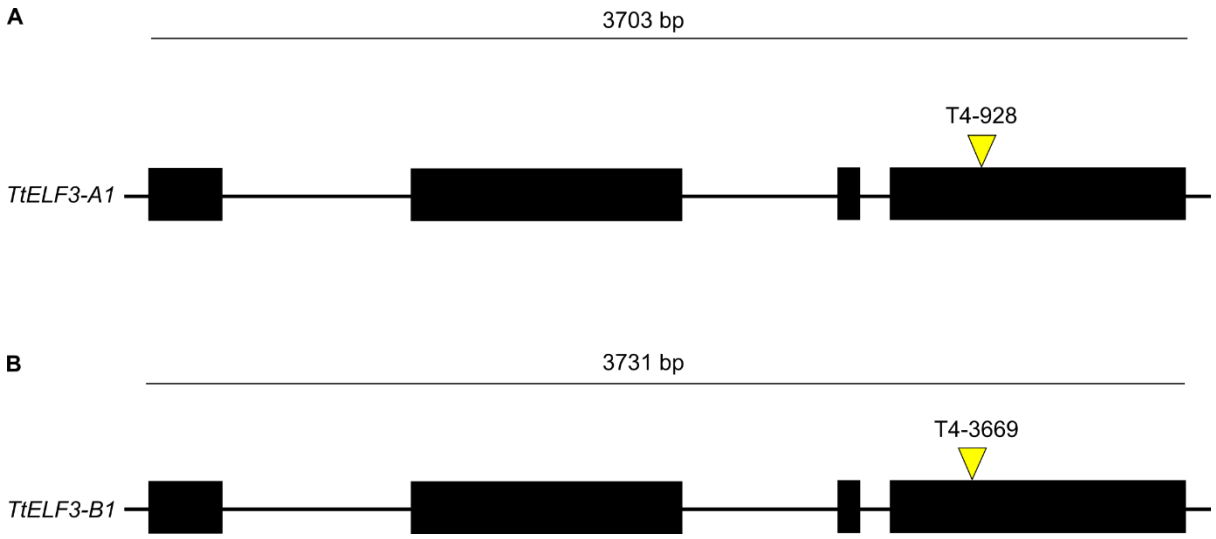

S6 Fig. The location of mutations within the A and B sub-genome copies of *TtELF3*.

(A-B) Scale diagram of (A) *TtELF3-A1* and (B) *TtELF3-B1* where black rectangles represent exons ordered 5'-3' (left-to-right), horizontal line above represents length of gene from start to stop codon (bp), space between exons represents introns. Yellow triangles denote the position of premature stop codons denoting the source TILLING line as annotated in (Alvarez *et al.* 2016).

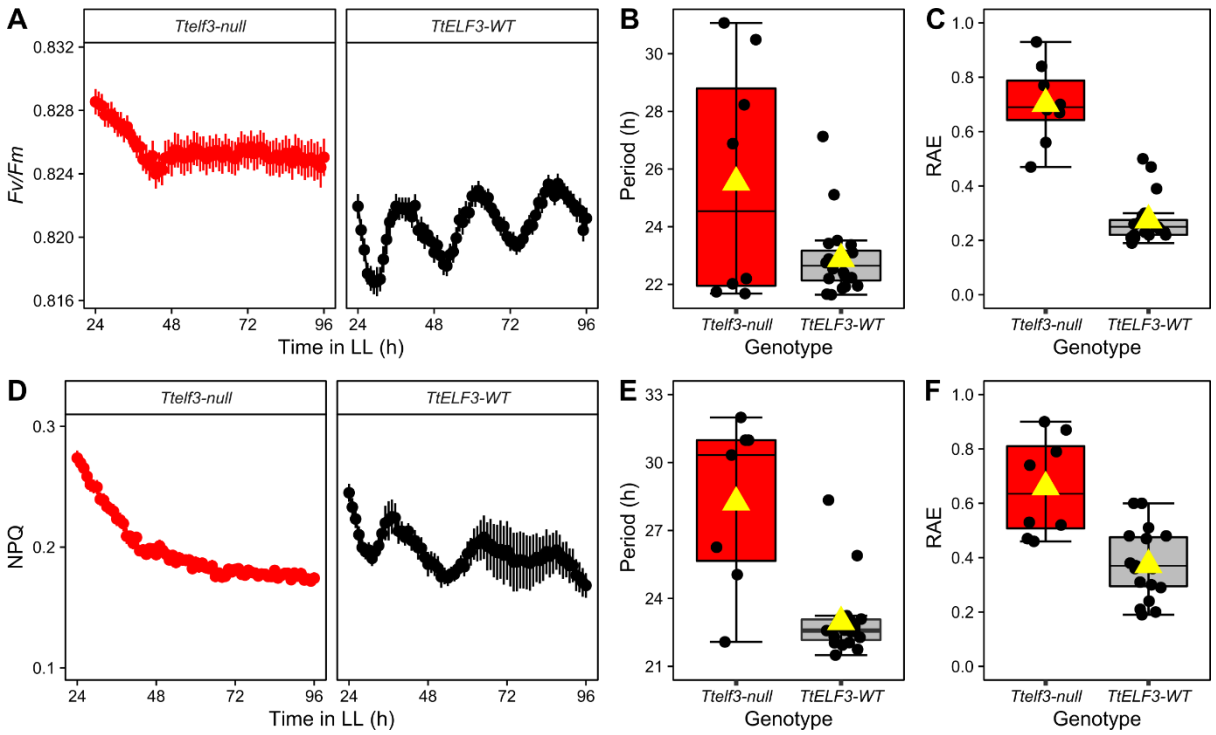

S7 Fig. *Ttelf3-null* is arrhythmic for PF parameters in LL.

(A) Mean F_v/F_m of *TtELF3*-WT (black) and *Ttelf3*-null (red) in LL (n = 24) (B) Mean period length (hours) and (C) RAE values for plot (A). (D) Mean NPQ of *TtELF3-WT* (black) and *Ttelf3*-null (red) in LL (n = 24) (E) Mean period length (hours) and (F) RAE values for plot (D). Error bars represent SEM. For plots (B), (C), (D) & (E) upper and lower hinges represent the first and third quartiles (25th and 75th percentiles), the middle hinge represents the median value, yellow triangle represents mean value and black dots represent individual replicates.

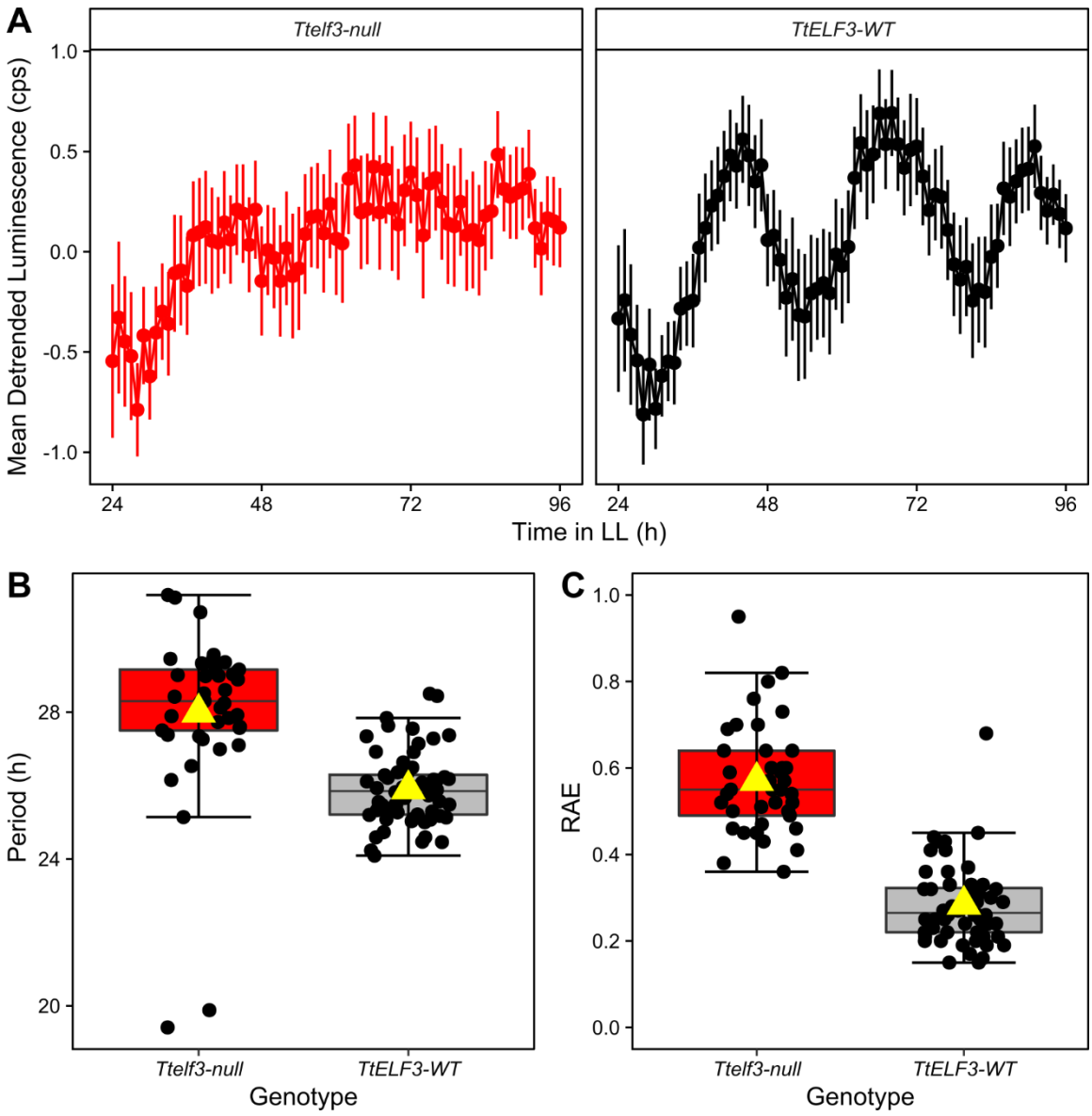

S8 Fig. *Ttelf3-null* is arrhythmic for DF in LL.

(A) Mean DF luminescence in counts per second (cps) normalised to -1 to 1 using Biodare2 with error bars representing standard deviation (n = *TtELF3*-WT 63, *Ttelf3*-null *72*). (B) Amplitude and (C) RAE for *TtELF3*-WT (black) and *Ttelf3*-null (red) in (A) calculated using FFT-NLLS fit in Biodare2 where upper and lower hinges represent the first and third quartiles (25th and 75th percentiles), the middle hinge represents the median value, yellow triangle represents mean value and black dots represent individual replicates.

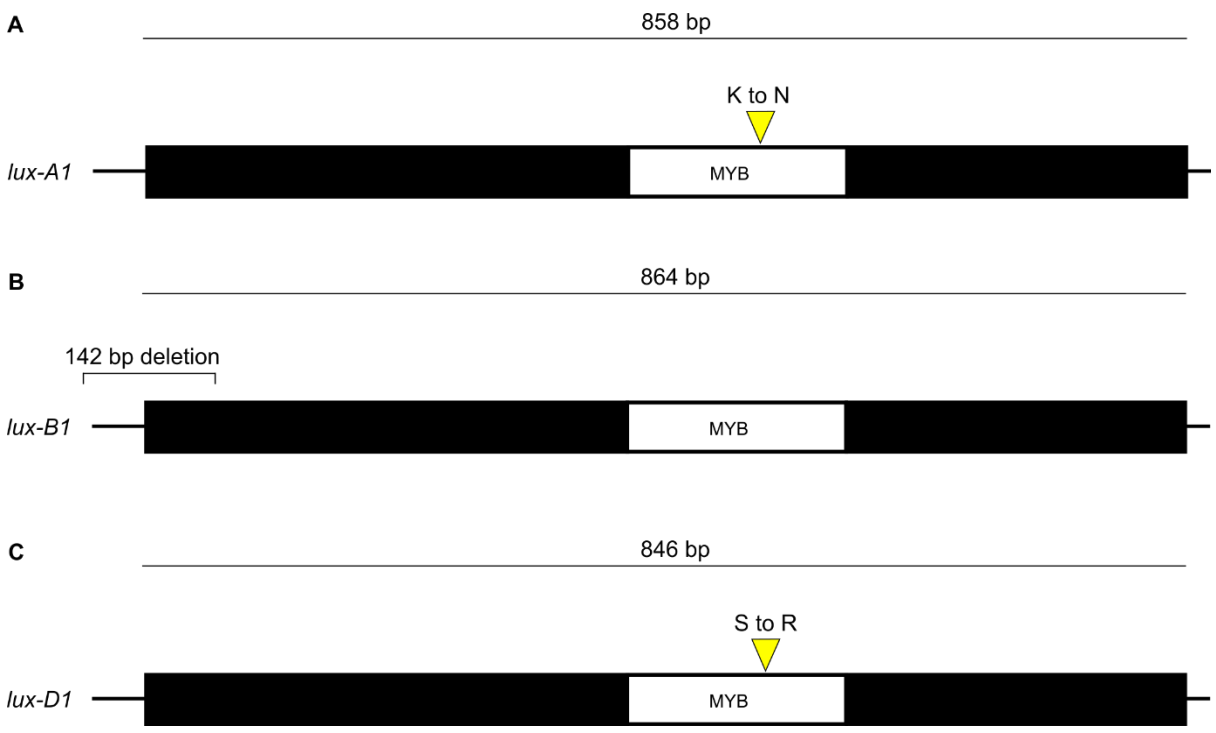

S9 Fig. The location of mutations in the different sub-genome copies of *LUX.*

(A-C) Diagram of the A sub-genome (A), B sub-genome (B) and D sub-genome (C) copies of *LUX* where black rectangle represents the *LUX* exon drawn 5' to 3' (left-to-right) and the embedded white rectangle denotes the highly conserved MYB-domain. Yellow triangles denote the location of amino acid substitution within the SHAQKYF motif (A, C). (B) line and annotation show the location of 142 bp deletion in the *lux-B1* allele (Mizuno *et al.* 2016).

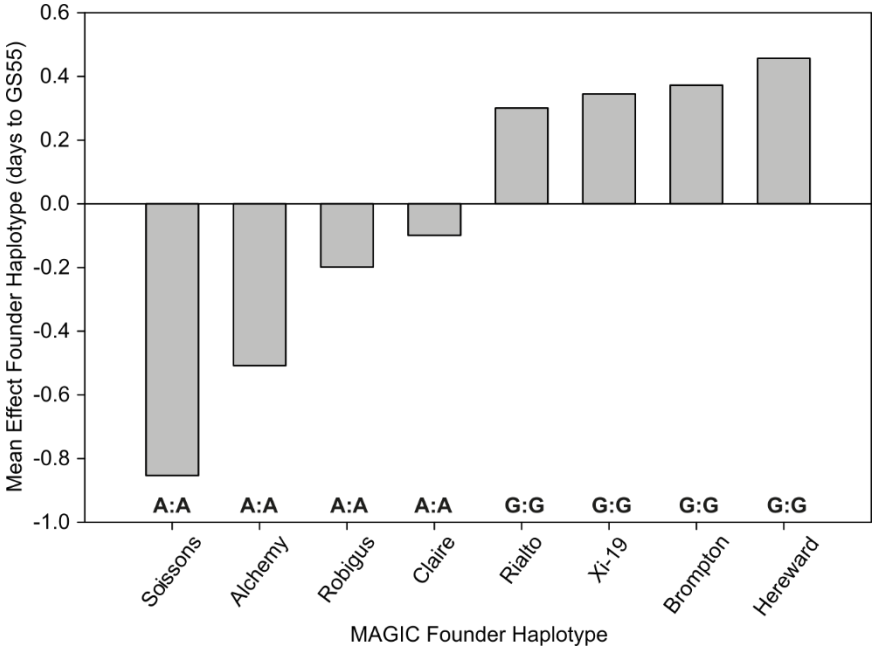

S10 Fig. The Ser674Gly SNP is a candidate for the causal *Eps-B1* SNP.

KASP Genotype association with MAGIC founder haplotype effects at the *Eps-B1* locus. Founder haplotype effects are calculated as the mean of the 2013 and 2014 founder effect. Genotype of A|A corresponds to homozygous for adenine, encoding the ancestral Serine, whilst G|G corresponds to homozygous guanine encoding the non-ancestral Glycine residue.

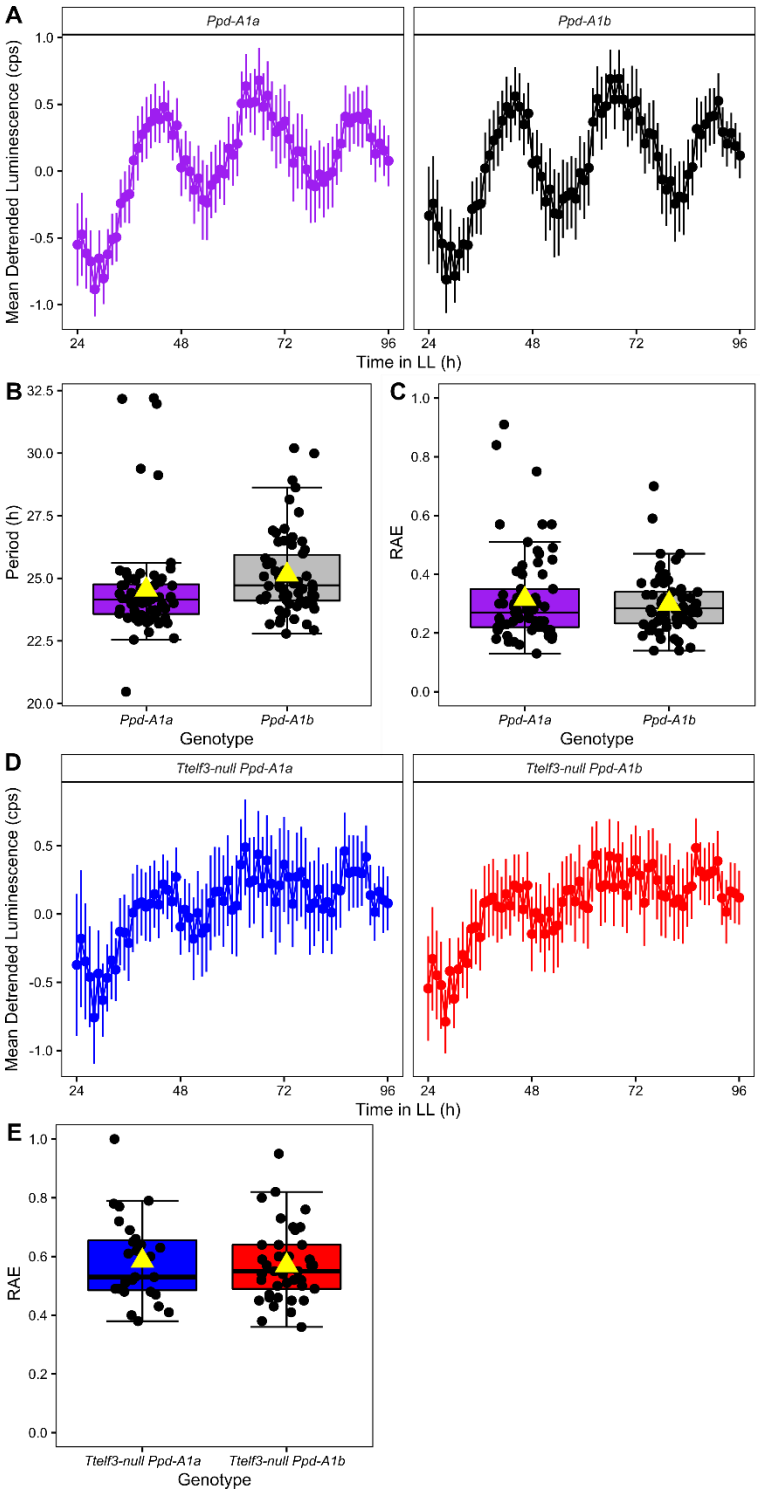

Figure S11 There is no significant difference between the circadian rhythms of kronos and *Ttelf3-null* lines containing the *Ppd-A1a* and *Ppd-A1b* alleles.

(A) Mean DF luminescence in counts per second (cps) normalised to -1 to 1 using Biodare2 with error bars representing standard deviation (n = *Ppd-A1a* 68, *Ppd-A1b* 62). (B) Amplitude and (C) RAE for *Ppd-A1a* (purple) and *Ppd-A1b* (black) in (A). (D) Mean DF luminescence in counts per second (cps) normalised to -1 to 1 using Biodare2 with error bars representing standard deviation (n = *Ttelf3-null Ppd-A1a* 66, *Ttelf3-null Ppd-A1b 22*) and (E) RAE for *Ttelf3-null Ppd-A1a* (blue) and *Ttelf3-null Ppd-A1b* (red). Amplitude and RAE calculated using FFT-NLLS fit in Biodare2 where upper and lower hinges represent the first and third quartiles (25th and 75th percentiles), the middle hinge represents the median

value, yellow triangle represents mean value and black dots represent individual replicates for plants where estimation was possible.

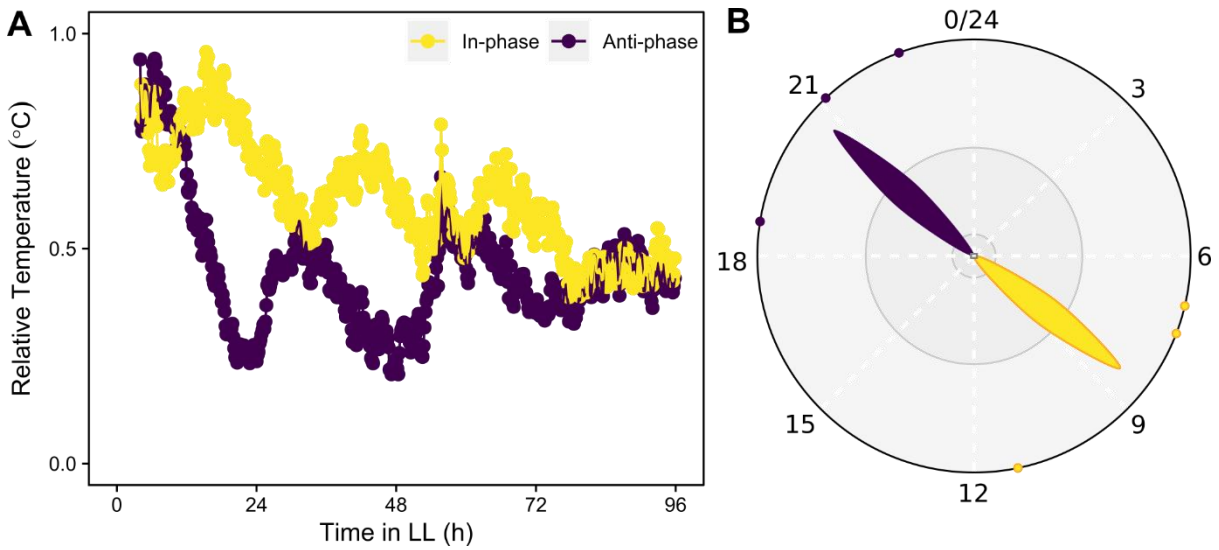

S12 Fig. In-phase and anti-phase leaf temperature rhythms in continuous light.

(A) Mean leaf temperature relative to background (n = 3) of four week old cadenza plants entrained to 16 h light:8 h dark cycles in-phase (yellow) or 16 h light: 8 h dark cycles that were 12 hours anti-phased (purple). (B) Phase plot of data shown in (A).

S1 Table: GS55 2012 QTLs

Output from the reanalysis of the NIAB 2012 GS55 data using MPWGAIM, originally analysed using Bayesian Networks (Scutari *et al.* 2014). Dist (cM) refers to the markers genetic mapping distance in centiMorgan. Founder corresponds to founder variety in alphabetical order (1 Alchemy, 2 Brompton, 3 Claire, 4 Hereward, 5 Rialto, 6 Robigus, 7 Soissons and 8 Xi-19). Size: Size of effect of each founder allele (days to GS55). LOGP is –log10(p) and corresponds to the overall significance of the QTL as a measure of its strength. Prob: probability QTL is from all founders shown (p). Founder LOGP and Founder Prob are LOGP and Prob for individual founders. % var is the percentage of genetic variance explained by each QTL.

Chr	Left Marker	dist (cM)	Right Marker	dist (cM)	Founder	Size	Founder Prob	Founder LOGP	Prob	% var	LOGP
1B	IAAV5516	297.84	BS00001128_51	298.34	1	-0.207	0.399	0.4	0.048	1.6	**1.32**
					2	0.946	0.077	1.11			
					3	0.112	0.445	0.35			
					4	0.318	0.304	0.52			
					5	0.698	0.148	0.83			
					6	-1.119	0.07	1.15			
					7	-1.185	0.021	1.67			
					8	0.437	0.259	0.59			
1D	Kukri_c2464_592	18.04	D_contig57829_235	18.21	1	-0.81	0.113	0.95	0.003	2.5	**2.59**
					2	-0.569	0.238	0.62			
					3	1.282	0.042	1.37			
					4	-1.024	0.066	1.18			
					5	0.631	0.27	0.57			
					6	0.849	0.12	0.92			
					7	-1.18	0.036	1.45			
					8	0.82	0.21	0.68			
1D	CAP11_c1157_168	100.79	Kukri_c29687_369	100.95	1	0.552	0.254	0.6	0.275	0.9	**0.56**
					2	0.105	0.446	0.35			
					3	-0.11	0.447	0.35			
					4	0.021	0.49	0.31			
					5	-0.044	0.477	0.32			

Chr	Left Marker	dist (cM)	Right Marker	dist (cM)	Founder	Size	Founder Prob	Founder LOGP	Prob	% var	LOGP
					6	0.003	0.498	0.3			
					7	0.734	0.134	0.87			
					8	-1.261	0.015	1.82			
2A	RAC875_c20273_823	35.38	BS00094817_51	35.88	1	0.45	0.218	0.66	0.035	1.6	**1.45**
					2	0.771	0.163	0.79			
					3	0.133	0.418	0.38			
					4	-1.126	0.032	1.5			
					5	-0.193	0.404	0.39			
					6	-1.262	0.019	1.71			
					7	0.739	0.11	0.96			
					8	0.487	0.241	0.62			
2B	BS00060618_51	317.61	BS00000012_51	318.61	1	0.176	0.417	0.38	0.049	1.6	**1.31**
					2	0.748	0.175	0.76			
					3	1.643	0.022	1.66			
					4	-0.88	0.107	0.97			
					5	-0.565	0.206	0.69			
					6	-0.392	0.267	0.57			
					7	-0.326	0.304	0.52			
					8	-0.404	0.265	0.58			
2D	Kukri_c27309_590	48.57	BS00064538_51	56.64	1	0.669	0.293	0.53	0	18.5	**18.33**
					2	2.727	0.009	2.03			
					3	0.215	0.44	0.36			
					4	1.112	0.211	0.68			
					5	0.759	0.276	0.56			
					6	0.897	0.245	0.61			
					7	-6.194	0	7.11			
					8	-0.185	0.437	0.36			
3A	wsnp_Ex_rep_c106152_90334299	78.8	Kukri_c51247_322	83.81	1	0.671	0.184	0.74	0.001	3	**2.84**
					2	-1.839	0.006	2.25			

Chr	Left Marker	dist (cM)	Right Marker	dist (cM)	Founder	Size	Founder Prob	Founder LOGP	Prob	% var	LOGP
					3	-0.671	0.187	0.73			
					4	0.716	0.155	0.81			
					5	-0.885	0.102	0.99			
					6	0.215	0.374	0.43			
					7	0.247	0.364	0.44			
					8	1.546	0.01	2.01			
3D	RAC875_c48773_253	31.11	RFL_Contig2471_119	31.28	1	-0.133	0.442	0.35	0.417	0.7	**0.38**
					2	0.159	0.431	0.37			
					3	-0.351	0.351	0.45			
					4	-0.525	0.276	0.56			
					5	-0.025	0.489	0.31			
					6	-0.443	0.244	0.61			
					7	1.191	0.021	1.68			
					8	0.128	0.423	0.37			
4A	BS00064140_51	133.18	BS00101512_51	134.18	1	0.521	0.273	0.56	0.002	2.4	**2.75**
					2	0.176	0.415	0.38			
					3	0.277	0.376	0.42			
					4	0.266	0.36	0.44			
					5	0.118	0.447	0.35			
					6	0.019	0.488	0.31			
					7	0.727	0.187	0.73			
					8	-2.104	0	3.63			
5B	BobWhite_c22572_782	196.48	Kukri_c836_513	196.65	1	-3.398	0.001	3.11	0	6	**3.85**
					2	0.725	0.232	0.63			
					3	0.886	0.158	0.8			
					4	1.621	0.088	1.05			
					5	-0.001	0.5	0.3			
					6	-1.505	0.037	1.43			
					7	0.704	0.206	0.69			

Chr	Left Marker	dist (cM)	Right Marker	dist (cM)	Founder	Size	Founder Prob	Founder LOGP	Prob	% var	LOGP
					8	0.968	0.141	0.85			
6B	wsnp_Ex_c12450_19850827	215.75	tplb0045b09_1555	216.42	1	0.089	0.461	0.34	0.269	1.1	**0.57**
					2	0.723	0.117	0.93			
					3	-0.552	0.264	0.58			
					4	0.368	0.333	0.48			
					5	-0.111	0.447	0.35			
					6	0.247	0.388	0.41			
					7	0.467	0.299	0.53			
					8	-1.232	0.02	1.71			
6D	BS00094895_51	124.37	GENE_4168_925	125.04	1	-0.044	0.472	0.33	0.169	1	**0.77**
					2	-0.093	0.449	0.35			
					3	0.85	0.082	1.09			
					4	-0.622	0.216	0.66			
					5	-0.674	0.198	0.7			
					6	0.592	0.169	0.77			
					7	-0.56	0.152	0.82			
					8	0.551	0.187	0.73			
7B	BS00036788_51	58.06	CAP7_c10566_170	58.22	1	-0.73	0.18	0.74	0.008	2.5	**2.09**
					2	-0.247	0.402	0.4			
					3	0.422	0.312	0.51			
					4	1.264	0.029	1.53			
					5	0.22	0.411	0.39			
					6	1.249	0.065	1.19			
					7	-0.704	0.173	0.76			
					8	-1.473	0.012	1.91			

S2 Table. The chr1B_685645813/ Ser674Gly SNP is globally rare. Wheat HapMap data of a diverse germplasm collection and the 10+ Wheat genome project (italics). UK varieties highlighted in bold. Genotype of A|A corresponds to homozygous for adenine at the Ser674Gly SNP encoding the ancestral serine whilst G|G corresponds to homozygous guanine encoding the non-ancestral glycine (red).

Variety	Genotype (forward strand)	Variety	Genotype (forward strand)	Variety	Genotype (forward strand)
93	A|A	*Jagger*	*A|A*	PI278297	A|A
102	A|G	*Julius*	*A|A*	PI349512	A|A
403	A|A	klein_chamaco	A|A	PI366716	A|A
407-IV_60	A|A	*Lancer*	*A|A*	PI366905	A|A
AC_Barrie	A|A	M6	A|A	PI382150	A|A
acc1	A|A	*Mace*	*A|A*	PI406517	A|A
acc2	A|A	Marquis	A|A	PI445736	A|A
acc3	A|G	Neepawa	A|A	PI470817	A|A
acc4	A|G	*Norin61*	*A|A*	PI477870	A|A
acc5	A|A	Opata	A|A	PI481718	A|A
Alabasskaja	A|A	***Paragon***	***G|G***	PI481923	A|A
Arina	*G|G*	pavon	A|A	PI565213	A|A
Avalon	**A|A**	pbw343	A|A	PI82469	A|A
Cadenza	***G|G***	PI153785	A|A	PI8813	A|A
CDC Landmark	*A|A*	PI166180	A|A	PR267	A|A
CDC Stanley	*A|A*	PI166333	A|A	rac875	A|A
chakwat86	A|A	PI177943	A|A	**Rialto**	**G|G**
cham6	A|A	PI185715	A|A	***Robigus***	***A|A***
Chinese Spring	A|A	*PI190962*	*A|A*	*Sy Mattis*	*A|A*
Claire	***A|A***	PI192001	A|A	**Taxi**	**A|A**
clear_white	A|A	PI192569	A|A	Truman	A|A
dharwar_dry	A|A	PI222669	A|A	Utmost	A|A
Estacao	A|A	PI245368	A|A	vorobey	A|A
hidhab	A|A	PI262611	A|A	*Weebil*	*A|A*

S3 Table. The Ser674Gly SNP segregates with heading date in UK varieties. Additional genotyping and heading information from Zikhali *et al*., 2016 (Zikhali *et al.* 2016) TGAC reference sequences (Clavijo *et al.* 2017). MAGIC founder varieties highlighted in bold, non-ancestral glycine in red.

Variety	Allele	Heading
Alchemy	A|A	early
Claire	A|A	early
Robigus	A|A	early
Avalon	A|A	early
Brompton	G|G	late
Hereward	G|G	late
Rialto	G|G	late
Xi-19	G|G	late
Paragon	G|G	NA
Cadenza	G|G	late
Spark	G|G	NA
Badger	G|G	NA
Savannah	G|G	NA

S4 Table. Haplotype analysis of the *TaELF3* region between exon 2 and exon 3 (see Fig 3). Variant location refers to position relative to Chinese spring *TaELF3-1D* transcription start site, first letter refers to base in Chinese Spring, second letter refers to changed base.

	ELF3-1D region	**Exon 2**	**Intron 2**																										
	Variant location	T1832C	C1933T	C1982T	A2028G	C2040A	A2046G	T2056G	A2084G	A2102G	G2104A	G2109C	C2128T	A2161G	2167-2471	T2483C	2504-2505	A2521G	2555	T2562C	2609	2613-2614	2616-2622	2625-2627	2633	2636-2637	G2646C	2651-2653
Cultivar	**Haplotype**	**Var 1**	**Var 2**	**Var 3**	**Var 4**	**Var 5**	**Var 6**	**Var 7**	**Var 8**	**Var 9**	**Var 10**	**Var 11**	**Var 12**	**Var 13**	**Var 14**	**Var 15**	**Var 16**	**Var 17**	**Var 18**	**Var 19**	**Var 20**	**Var 21**	**Var 22**	**Var 23**	**Var 24**	**Var 25**	**Var 26**	**Var 27**
Alchemy	H1	T	C	C	A	C	A	T	A	A	G	G	C	A	Ins	T	-	A	-	T	G	GT	Ins	Ins	A	CT	G	CAA
ArinaLrFor	H1	T	C	C	A	C	A	T	A	A	G	G	C	A	Ins	T	-	A	-	T	G	GT	Ins	Ins	A	CT	G	CAA
Brompton	H1	T	C	C	A	C	A	T	A	A	G	G	C	A	Ins	T	-	A	-	T	G	GT	Ins	Ins	A	CT	G	CAA
Cadenza	H2	C	T	T	G	A	G	G	G	G	A	C	T	G	Del	C	AG	G	T	C	-	-	Del	Del	-	-	C	TGG
Chinese Spring	H1	T	C	C	A	C	A	T	A	A	G	G	C	A	Ins	T	-	A	-	T	G	GT	Ins	Ins	A	CT	G	CAA
Claire	H1	T	C	C	A	C	A	T	A	A	G	G	C	A	Ins	T	-	A	-	T	G	GT	Ins	Ins	A	CT	G	CAA
Hereward	H1	T	C	C	A	C	A	T	A	A	G	G	C	A	Ins	T	-	A	-	T	G	GT	Ins	Ins	A	CT	G	CAA
Jagger	H2	C	T	T	G	A	G	G	G	G	A	C	T	G	Del	C	AG	G	T	C	-	-	Del	Del	-	-	C	TGG
Julius	H1	T	C	C	A	C	A	T	A	A	G	G	C	A	Ins	T	-	A	-	T	G	GT	Ins	Ins	A	CT	G	CAA
Landmark	H1	T	C	C	A	C	A	T	A	A	G	G	C	A	Ins	T	-	A	-	T	G	GT	Ins	Ins	A	CT	G	CAA
Mace	H1	T	C	C	A	C	A	T	A	A	G	G	C	A	Ins	T	-	A	-	T	G	GT	Ins	Ins	A	CT	G	CAA
Norin61	H1	T	C	C	A	C	A	T	A	A	G	G	C	A	Ins	T	-	A	-	T	G	GT	Ins	Ins	A	CT	G	CAA
Paragon	H1	T	C	C	A	C	A	T	A	A	G	G	C	A	Ins	T	-	A	-	T	G	GT	Ins	Ins	A	CT	G	CAA
Rialto	H1	T	C	C	A	C	A	T	A	A	G	G	C	A	Ins	T	-	A	-	T	G	GT	Ins	Ins	A	CT	G	CAA
Robigus	H1	T	C	C	A	C	A	T	A	A	G	G	C	A	Ins	T	-	A	-	T	G	GT	Ins	Ins	A	CT	G	CAA
Soissons	H1	T	C	C	A	C	A	T	A	A	G	G	C	A	Ins	T	-	A	-	T	G	GT	Ins	Ins	A	CT	G	CAA
Spark	H2	C	T	T	G	A	G	G	G	G	A	C	T	G	Del	C	AG	G	T	C	-	-	Del	Del	-	-	C	TGG
Stanley	H1	T	C	C	A	C	A	T	A	A	G	G	C	A	Ins	T	-	A	-	T	G	GT	Ins	Ins	A	CT	G	CAA
SyMattis	H1	T	C	C	A	C	A	T	A	A	G	G	C	A	Ins	T	-	A	-	T	G	GT	Ins	Ins	A	CT	G	CAA
Weebil	H1	T	C	C	A	C	A	T	A	A	G	G	C	A	Ins	T	-	A	-	T	G	GT	Ins	Ins	A	CT	G	CAA
Xi-19	H2	C	T	T	G	A	G	G	G	G	A	C	T	G	Del	C	AG	G	T	C	-	-	Del	Del	-	-	C	TGG

S5 Table. Alignment of 300kb surrounding *ELF3-1D* in 10+ wheat genome lines. Average nucleotide identity scores from alignment of 300kb sequence surrounding *ELF3-1D* in the 10+ wheat genome cultivars. Alignment produced using the whole genome alignment tool from CLC workbench 21.0.3 using a 15-base seed with no mismatches.

Cultivar	ArinaLrFor	CDC_Landmark	CDC_Stanley	Lancer	Mace	Norin61	CSv1.0	Julius	SYMattis	Jagger	Cadenza
ArinaLrFor	100.00	99.82	99.94	99.90	99.95	99.81	99.89	99.93	99.97	91.00	91.44
CDC_Landmark	99.82	100.00	100.00	99.89	99.85	99.93	99.82	99.90	99.94	90.57	91.44
CDC_Stanley	99.94	100.00	100.00	99.89	99.95	99.97	99.89	99.92	99.94	90.76	91.44
Lancer	99.90	99.89	99.89	100.00	99.94	99.92	99.91	99.94	99.93	91.00	91.42
Mace	99.95	99.85	99.95	99.94	100.00	99.90	99.86	99.98	99.98	90.51	91.44
Norin61	99.81	99.93	99.97	99.92	99.90	100.00	99.95	99.93	99.95	91.01	91.43
CSv1.0	99.89	99.82	99.89	99.91	99.86	99.95	100.00	99.93	99.83	91.00	91.44
Julius	99.93	99.90	99.92	99.94	99.98	99.93	99.93	100.00	99.99	91.00	91.43
SYMattis	99.97	99.94	99.94	99.93	99.98	99.95	99.83	99.99	100.00	91.00	91.43
Jagger	91.00	90.57	90.76	91.00	90.51	91.01	91.00	91.00	91.00	100.00	99.94
Cadenza	91.44	91.44	91.44	91.42	91.44	91.43	91.44	91.43	91.43	99.94	100.00

Internal

S6 Table. Promoter motif analysis of *TtELF3.* Column A refers to the A sub-genome, B sub-genome and D to the D sub-genome. Motifs and corresponding sequences taken from (Wang *et al.* 1997, Gendron *et al.* 2012, Huang *et al.* 2012).

Motif	Abbreviation	Sequence	A	B	D	Arabidopsis
Evening element	EE	AAAATATCT	0	1	0	0
Evening Like element	ELE	AATATCT	1	0	0	1
CCA1 binding site (A variant)	/	AAAAATCT	0	0	0	0
CCA1 binding site (C variant)	/	AACAATCT	0	0	0	2
Morning element 1	ME 1	CCACAC	0	1	1	0
Morning element 2	ME 2	GTGTGG	1	1	2	0
Hormone Up at Dawn 1	HUD 1	CACATG	2	3	4	2
Hormone Up at Dawn 2	HUD 2	CATGTG	3	9	6	0
G BOX (morning)	/	CACGTG	1	0	3	0
GATA (evening)	/	GGATA	4	8	6	6
Starch box (midnight)	/	AAGCCC	1	0	1	0
Telo-Box (midnight)	/	AAACCCT	2	0	0	0
Protein Box (midnight)	/	ATGGGCC	0	2	1	0

Internal

S7 Table. Promoter motif analysis of *TtLHY.* Column A refers to the A sub-genome, B sub-genome and D to the D sub-genome. Motifs and corresponding sequences taken from (Wang *et al.* 1997, Gendron *et al.* 2012, Huang *et al.* 2012).

Motif	Abbreviation	Sequence	A	B	D	Arabidopsis
Evening element	EE	AAAATATCT	0	0	0	0
Evening Like element	ELE	AATATCT	0	0	0	0
CCA1 binding site (A variant)	/	AAAAATCT	0	1	0	0
CCA1 binding site (C variant)	/	AACAATCT	1	0	0	0
Morning element 1	ME 1	CCACAC	1	1	1	1
Morning element 2	ME 2	GTGTGG	2	0	0	0
Hormone Up at Dawn 1	HUD 1	CACATG	1	1	1	1
Hormone Up at Dawn 2	HUD 2	CATGTG	4	3	3	0
G BOX (morning)	/	CACGTG	1	1	0	1
GATA (evening)	/	GGATA	3	3	3	3
Starch box (midnight)	/	AAGCCC	0	0	1	1
Telo-Box (midnight)	/	AAACCCT	0	0	0	0
Protein Box (midnight)	/	ATGGGCC	0	1	1	0

Internal

S8 Table. Promoter motif analysis of *TtLUX.* Column A refers to the A sub-genome, B sub-genome and D to the D sub-genome. Motifs and corresponding sequences taken from (Wang *et al.* 1997, Gendron *et al.* 2012, Huang *et al.* 2012).

Motif	Abbreviation	Sequence	A	B	D	Arabidopsis
Evening element	EE	AAAATATCT	9	4	4	1
Evening Like element	ELE	AATATCT	3	1	1	2
CCA1 binding site (A variant)	/	AAAAATCT	1	0	0	2
CCA1 binding site (C vairiant)	/	AACAATCT	0	1	0	0
Morning element 1	ME 1	CCACAC	1	1	1	0
Morning element 2	ME 2	GTGTGG	1	1	0	0
Hormone Up at Dawn 1	HUD 1	CACATG	2	1	2	0
Hormone Up at Dawn 2	HUD 2	CATGTG	2	2	0	1
G BOX (morning)	/	CACGTG	2	3	2	2
GATA (evening)	/	GGATA	3	5	2	2
Starch box (midnight)	/	AAGCCC	0	0	2	0
Telo-Box (midnight)	/	AAACCCT	3	2	1	2
Protein Box (midnight)	/	ATGGGCC	1	1	2	0

Internal

S9 Table. Total number of SNPs within the coding sequence of *ELF3* in the 10+ Wheat Genomes project cultivars. A SNP was recorded if the base was different to the Chinese Spring IWGSCRefseqv1.1 sequence in the alignment. SNPs within the same codon were recorded individually. It was not possible to create clear alignments between *ELF3-1D* Chinese Spring, Jagger and Cadenza and so the coding sequence for the three cultivars was downloaded from ENSEMBL plants, aligned and the number of SNPs manually counted. NS = non-synonymous SNP, S= synonymous SNP, PAV = presence/absence variation. Cultivars were considered to share the same allele if the CDS was identical. Zavitan is a tetraploid variety and so lacks a D sub genome.

	Chromosome					
	1A		**1B**		**1D**	
Cultivar	**NS**	**S**	**NS**	**S**	**NS**	**S**
ArinaLrFor	2	2	1	0	0	0
CDC Stanley	2	2	0	0	0	0
CDC Landmark	2	2	0	0	0	0
Cadenza	0	1	1	0	35	23
Claire	0	1	0	0	0	0
Jagger	2	3	0	1	35	23
Julius	PAV	PAV	0	0	1	0
Lancer	2	2	0	0	0	0
Norin61	2	2	0	0	0	0
Mace	2	2	0	0	0	0
PI190962	0	0	0	0	0	0
Paragon	0	1	1	0	0	0
Robigus	0	0	0	0	0	0
SY Mattis	0	1	0	0	0	0
Zavitan	7	2	1	3	*NA*	*NA*
Total No. SNP's	21	21	3	4	71	46
Total No. Alleles	5		3		3	

Internal